NBSIR 82-2611

Development of the Cone Calorimeter -- A Bench-Scale Heat Release Rate Apparatus Based on Oxygen Consumption

U.S. DEPARTMENT OF COMMERCE
National Bureau of Standards
Center for Fire Research
Washington, DC 20234

November 1982

U.S. DEPARTMENT OF COMMERCE
NATIONAL BUREAU OF STANDARDS

NBSIR 82-2611

DEVELOPMENT OF THE CONE CALORIMETER -- A BENCH-SCALE HEAT RELEASE RATE APPARATUS BASED ON OXYGEN CONSUMPTION

Vytenis Babrauskas

U.S. DEPARTMENT OF COMMERCE
National Bureau of Standards
Center for Fire Research
Washington, DC 20234

November 1982

U.S. DEPARTMENT OF COMMERCE, Malcolm Baldrige, *Secretary*
NATIONAL BUREAU OF STANDARDS, Ernest Ambler, *Director*

TABLE OF CONTENTS

LIST OF TABLES

LIST OF FIGURES

NOMENCLATURE

A_s - specimen exposed surface area (m^2)

b - stoichiometric factor (--)

C - orifice meter calibration constant ($m^{1/2}\ kg^{1/2}\ K^{1/2}$)

F - view factor (--)

Δh_c - net heat of combustion (kJ/kg)

M - molecular weight (g/mol)

$\dot{m}$ - mass flow (kg/s)

$\dot{n}$ - mole flow (mol/s)

ΔP - orifice meter pressure differential (p_a)

$\dot{q}$ - heat rate (kW)

$\dot{q}''$ - heat per unit area (kW/m^2)

r_o - stoichiometric oxygen/fuel mass ratio (--)

t - time (s)

Δt - time increment (s)

T_e - temperature for orifice meter (K)

X - mole fraction (--)

β - oxygen analyzer response parameter (s^{-1})

ε - emissivity (--)

σ - Stefan-Boltzmann constant (5.67×10^{-11} kW $m^{-2}K^{-4}$)

Subscripts

air - air

CO_2 - carbon dioxide

e - exhaust

f - fuel

g - gage

h - heater

O_2 - oxygen

p - pyrolysis

∞ - ambient conditions

Superscript

^{o} - baseline value (before test)

DEVELOPMENT OF THE CONE CALORIMETER -- A BENCH-SCALE HEAT RELEASE RATE APPARATUS BASED ON OXYGEN CONSUMPTION

Vytenis Babrauskas

National Bureau of Standards
Washington, D.C. 20234

A new bench-scale rate of heat release calorimeter utilizing the oxygen consumption principle has been developed for use in fire testing and research. Specimens may be of uniform or composite construction and may be tested in a horizontal, face-up orientation, or, for ones which do not melt, also vertically oriented. An external irradiance of zero to over 100 kW/m^2 may be imposed by means of a temperature-controlled radiant heater. The rate of heat release is determined by measuring combustion product gas flow and oxygen depletion, while the mass loss is simultaneously recorded directly. The instrument has been designed to be capable of higher accuracy than existing instruments and yet to be simple to operate and moderate in construction cost. The instrument is termed a "cone calorimeter" because of the geometric arrangement of the electric heater.

Keywords: Combustion of plastics; combustion properties; fire tests; heat of combustion; ignitability; oxygen consumption; rate of heat release.

1. INTRODUCTION

In a building fire the rate of heat release from burning combustibles is the quantity of most concern in predicting the course of the fire and its effects. Measurement techniques for determining the heat release rate of an arbitrary, full-sized combustible assembly are difficult and are just now beginning to be implemented. For instance, a technique [1]* was recently

* Numbers in brackets refer to literature references at the end of this paper.

developed for measuring the rate of heat release of full-sized furniture items. Even though full-scale measurement is possible in this case, it is much more convenient to do studies in a bench-scale apparatus. The rate of heat release of a full-scale item can conceptually be approximated by the use of data from certain bench-scale measurements:

(1) Ignitability (time to ignition at a specified irradiance)--This effect is not important in a deterministic scheme for the first item to ignite, but is important in a stochastic model and also for additional burning items.

(2) Surface Flame Spread Rate and Available Surface Area--The heat released has to be proportional to the amount of material exposed to fire, for which flame spread rates and corresponding burning areas are needed.

(3) Heat Release Rate per Unit Area--This number can be measured using a bench-scale test and approximates the heat release rate of a surface element of the full-scale object.

For some classes of objects ignitability and flame spread effects are known to be not significant. In those cases we correctly expect that the full-scale rate of heat release, $\dot{q}$, is proportional to the bench-scale, $\dot{q}''$, taken per unit area [2]. The relationship depends on a proportionality, at present empirical, which has to be established for a particular fire scenario. This proportionality can be dependent on the thickness, area, and mass of the full-scale items.

While the state of the art is just now emerging that will permit detailed advantage to be taken of the rate of heat release values, their basic importance has long been recognized and measurements of this type were being made as early as 1959 [3]. At the National Bureau of Standards (NBS) we have for some time felt the need for a small, bench-scale rate of heat release calorimeter which would incorporate features not available together in existing designs. We can first list the general attributes, commonly desired for any laboratory test method:

- Method to be quantitative
- Validity and accuracy
- Precision, repeatability, and reproducibility
- Ease of calibration
- Ease of specimen preparation
- Ease of data analysis and interpretation
- Low cost of apparatus
- Short preparation and testing time
- Ruggedness of apparatus
- Ease of physical installation and provision of utilities.

To this general list we can now add features specifically desired in a new heat release rate apparatus:

- Use of the oxygen-consumption technique, rather than measuring sensible heat
- Electric radiant heater (to avoid oxygen consumption from a fuel-burning heater itself)
- Simple and affordable enough to be useful for testing laboratories
- Square specimens (for preparation convenience)
- Suitable for both uniform and composite materials

- Irradiance adjustable over zero to 100 kW/m^2, to replicate a wide range of fire conditions

- Specimens to be tested in horizontal or vertical orientation; those which melt and drip to be tested horizontally only

- Irradiance to be easily calibratable before each test

- Irradiance uniformity

- Variable specimen thickness to be accommodated

- Specimen to be easily insertable and removable

- Specimen field of view to consist primarily of
  a) Temperature-controlled radiant heater, or
  b) Water-cooled surfaces, or
  c) Open air

- Specimen flames not to be appreciably deflected from natural flow

- Apparatus to also be usable for ignitability studies

- Electric spark ignition

- Sample mass loss measurement system (used for computing effective heat of combustion)

- Calibration procedure to be simple (to be done daily)

- Data presentation directly in kW/m^2

- Ease of maintainability and cleanability.

2. DISCUSSION OF REQUIREMENTS

At NBS we have had direct experience with four rate of heat release calorimeters. The original NBS calorimeter, "NBS-I," was conceived and designed by A. F. Robertson, then developed and described by Parker and Long in the early 1970's [4]. Eventually a larger redesigned and improved version, "NBS-II," was developed by Tordella [5]. More recently, feasibility of bench-scale oxygen consumption techniques was investigated by Sensenig [18], and a small developmental rate of heat release calorimeter based on oxygen consumption was constructed by Lawson [6] for testing building materials in the vertical orientation. Finally, we operated the Ohio State University (OSU) apparatus [7] and explored in detail some of its calibration difficulties [8].

The primary purpose of all these calorimeters is to measure the heat release rate of products in order to estimate their contribution to a room fire (as opposed to characterizing in detail their combustion chemistry behaviors). Since the primary purpose in the present case is to be repetitive product testing, certain features, such as ruggedness and modest cost, assume a top priority, while others, which are only useful for research studies, such as availability of redundant measurement paths, are considered of lower importance. None of the calorimeters listed above were considered to possess all the desired features; the most nearly adequate one, the NBS-II was also extremely costly. Thus, a discussion of the reasoning why the listed features are desired is appropriate.

Much of testing in existing instruments has been done on specimens in a vertical orientation, although horizontal specimen mounting has one distinct advantage: no specimens fall down or melt and run away when tested horizontally, but many do in the vertical position. While some arguments can even be made for testing exclusively in a horizontal orientation, it is clear that the capability of testing horizontal specimens is at least as important as testing vertical ones. Thus, the performance in the horizontal orientation was considered crucial.

The apparatus is intended for testing combustible materials used in furnishings, wall linings and other applications in buildings. Almost invariably these products are composite assemblies, rather than homogeneous substances. While some fire contribution of individual component materials can be recognized, the heat release behavior of a composite cannot be computed from data on the individual materials. Thus, specimens should be useable which are cut out through the thickness of manufactured goods. For convenience a square shape is preferable.

Heat release rate can be measured simply by sensing the outflow enthalpy directly by recording exhaust gas flow temperature rise. Experience indicates that this is subject to large heat-storage errors. An improved technique involves a substitution burner set to maintain a constant heat balance [4]. This is effective but costly and complex. To be preferred, instead is the principle of oxygen consumption measurement [9]. This is especially simple since oxygen is neither stored nor lost along the apparatus flow path. Also, packaged instruments for measuring O_2 concentrations are readily available and, unlike heat sensing methods, do not have to be developed. At NBS, oxygen consumption measurements in the NBS-II calorimeter were first made in 1978. A prototype small vertical O_2 calorimeter was also built here during 1978-79. Similar approaches have recently also been pursued in European laboratories where Svensson and Östman [10], Holmstedt [11], and Bluhme [12] have reported recent applications.

Most existing calorimeters are subject to irradiance errors, especially at higher irradiances or for larger samples. A burning specimen establishes a flame which can heat up internal apparatus surfaces. These heated surfaces can then radiate back to the specimen and introduce an unexpected and unknown increase in irradiance. Three techniques are available for minimizing this error. All internal apparatus surfaces which can irradiate the specimen should be (1) temperature controlled, or (2) water-cooled, or (3) far away.

To make reasonable analysis of results possible, an electric pilot ignitor arrangement should be used since it imposes no additional, localized heat flux upon the specimen and does not consume oxygen. Electric spark ignition was found, in addition, to be simpler and more reliable than a gas pilot.

Some existing calorimeters show substantial variations in the irradiance across the specimen face from the heater. This is undesirable both because average values become difficult to determine and because unexpected combustion changes can be introduced by local hot spots. A uniformity of the order of 15% should be readily achievable with careful design.

Gas burners are undesirable if the specimen irradiance is to be smoothly adjustable down to zero external flux. They are also undesirable in oxygen-consumption work because they introduce extraneous oxygen depletion. Electric heaters are not subject to these limitations. However, electric heaters, if located far away from the specimen, may be sizeable and consequently to consume excessive power. A suitable design requires a compact heater which can be powered from available laboratory mains.

The design of the apparatus has to be such that a valid measurement is maintained for all types of responses. Known pitfalls in this area with other equipment include radiation errors introduced when measuring specimens having flames of high emissivity and errors due to instrument time response problems. Use of oxygen consumption as a measurement technique is highly useful because it minimizes these difficulties.

For consistent operation, instrument calibration should be re-checked regularly. This suggests the usefulness of an arrangement where a calibration burner can be operated simply, without the need for re-installing one each time.

Experience suggests that ease of specimen insertion is an important factor to be considered in design. Quick and simple insertion should be possible in order to minimize starting time uncertainties.

The upper limit of specimen irradiance should be high enough to simulate required full-scale heat fluxes, with special attention to the more fire resistive materials. A value of at least 100 kW/m^2 is desirable and achievable.

Last but not least, for the instrument to be truly useful it has to be rugged. Sufficiently heavy duty materials and construction should be used to ensure that operating conditions do not change, leaks do not occur, warpage does not prevent a good fit, and similar problems do not cause erratic operation.

3. THE PRINCIPLE OF OXYGEN CONSUMPTION

The net heats of combustion for common organic materials range from very small up to about 50 MJ/kg. (Hydrogen, a special case, gives 120 MJ/kg). It has occasionally been observed that the heat of combustion released per kg of oxygen consumed is a nearly constant number. Huggett [9] has examined a wide variety of fuels and concluded that $\Delta h_c / r_o = 13.1 \times 10^3$ kJ/kg represents a value typical of most combustibles, including gases, liquids, and solids.

To implement this principle it would be necessary only to measure the total mass flow of oxygen in the combustion products and to compare that to the initial inflow, that is

$$\dot{q} = \frac{\Delta h_c}{r_o} (\dot{m}_{O_2,\infty} - \dot{m}_{O_2})$$

where the subscript ∞ denotes baseline ambient condition prior to start of test. From the form of this expression it can be seen that it does not matter at what speed the products are exhausted or how much excess air is pulled through. It is as if we were interested only in counting oxygen "holes".

4. APPARATUS DESIGN

4.1 Basic Apparatus Design (Figures 1 to 5, and Table 1)

Two features represented pivotal choices in the design of the calorimeter. It was first decided that oxygen consumption would be the method of measurement. In addition to the considerations given above, this has the advantage that when an electrical radiant source is used, no compensation is required for changes in heater power; that is, oxygen measurements are unaffected when the specimen flames raises the temperature of the radiant

source, and the temperature controller, in turn, reduces power to maintain constant heater temperature.

The second primary choice was the design of the radiation source. It was concluded that the simplest instrument design would involve an open construction, not involving an air-tight box. This, again, is readily possible only with the oxygen consumption technique (if sensible enthalpy were measured, radiated heat would not be captured). The radiant heater itself, for reasons of efficiency, should have the largest possible view factor and the smallest surface area. In addition, the heater should not be so located as to significantly disturb the flame flow pattern. Numerous alternatives were considered; the design that seemed best suited was a modified version of the ISO heater cone used in an ignitability test [13]. For a horizontal specimen this truncated cone shape appears to be the ideal configuration. More flexibility as to heater shape is available when burning samples vertically. However, for simplicity of operation it is easiest to use the same heater and merely to pivot it 90^0 into a vertical orientation.

The requirements for the exhaust/sampling system may then be stated. The hood must collect all the combustion products. The flow stream must be mixed and straightened. Oxygen sampling should be done with a multi-point probe in a region of well-developed flow. The probe should be arranged to minimize the possibility of clogging by soot. A controllable adjustment of the flow is desirable to optimize resolution. A provision is necessary, in any case, to measure the flow velocity and temperature in order to determine the exhaust mass flow.

4.2 Oxygen Sampling System (Figures 6 to 8)

The unusual aspects of oxygen measurements in this application are that only a small range, approximately 21 to 18% of oxygen concentration is used. This contrasts sharply to instrumenting room fire tests for oxygen, where the whole range of 21% to 0% can be expected. For calorimeter use, therefore, requirements are placed on stability and low noise for the oxygen meter which are quite strict. Instrument noise and short-term drift have to be kept to below approximately $\pm$ 0.005% O_2 to make the measurement feasible. Our

investigations at NBS led us to conclude that electrochemical or zirconium oxide type oxygen meters would not give sufficient stability and that a paramagnetic oxygen analyzer is necessary for this application.

In addition to the need for a high stability O_2 meter, the other portions of the gas sampling train have to be carefully designed and set up since any drift or flow fluctuations can show up as pressure variations at the inlet or the outlet of the O_2 meter and, therefore, appear as noise or error.

At the outlet end, changes in barometric pressure introduce an undesirable baseline shift, which is serious because of the narrow operating range. This difficulty is solved by putting an absolute back-pressure regulator on the outflow port of the oxygen analyzer. For proper operation this regulator should be located in a constant temperature environment.

At the inlet end, the gas sample is first drawn in to the system through a ring probe in the exhaust duct (Fig. 6). The probe has numerous holes facing away from the incident flow direction. A forward-facing probe is not viable due to soot clogging. Multiple holes are provided to permit the best possible averaging over any local fluctuations.

From the probe the sample goes through a soot filter to a cold trap to remove moisture (Fig. 7). Several designs were tried for this. A thermoelectric trap (Fig. 8) was designed since it has the advantage of continuous operation and can readily be electrically adjusted to the proper operating point. The cold trap outflow is equipped with a thermocouple, which should register slightly below 0^0C. For the design developed, typically 8 to 10 volts across the two thermoelectric modules is required. The water condenses into the separation chamber and is removed at the drain valve. From the cold trap the sample goes through the pump, at the exit of which is fitted a small surge tank to minimize downstream pressure fluctuations. At this point the major part of the flow goes through a relief pressure regulator and is wasted. Such an arrangement helps minimize transit time. The remaining flow passes through a drying cartridge, a CO_2 removal cartridge, a flow regulator, a 7 μm filter and into the oxygen analyzer. The drying cartridge is provided as back-up to the cold trap, in case of trap malfunction. The CO_2

removal cartridge is used to permit simplified data analysis. The flow regulator is necessary to reduce inlet pressure fluctuations with aging of the cartridges. The 7 μm filter is recommended for the protection of the oxygen analyzer cell.

4.3 Cone Heater (Figures 10 to 12)

In principle and in dimensions the cone heater follows closely the ISO heater [13]. The heater is constructed in the following way. An outer shell is welded to the top plate, which in turn is attached to the sliding hinged support. An inner shell is then inserted inside the outer shell, with a layer of low density refractory fiber blanket separating the two. This provides a double-wall construction to minimize heat radiation to the far side. The heater element (table 1) consists of a resistance heating wire packed in MgO refractory and swaged in a high-temperature alloy sheath. The element is wound into a cone shape using a winding mandrel (Fig. 12) attached to a lathe, clamping one end to the retaining plate and winding slowly by hand. A total of 7-1/2 tightly packed turns are wound, leaving about 45 mm free ends. The heater is inserted in the shell assembly and held in with a base plate (Fig. 11). The base plate also acts as a stop in setting the horizontal position level and holds brackets for spark plug (bracket A in horizontal testing, bracket B in vertical testing) and for calibration burner/heat flux gauge. Both the calibration burner and the heat flux gauge use the square opening in bracket A. The burner is oriented to discharge upwards.

The cone heater is mounted on a piano hinge to a sliding support bracket (Fig. 13) which slides on polytetrafluoroethylene (PTFE) sleeves and is secured with two thumbscrews to the main support rods (Fig. 14). A supplementary lock bracket (Fig. 13) is used to retain the cone when in a vertical position.

The heater element is described in table 1. Power is controlled by an electronic temperature controller using three thermocouples wired in parallel, located on the heater. Two different arrangements for thermocouples have been tried--(1) thermocouples welded to the inside of the inner cone shell, and (2) thermocouples looped around the heater element, with the bead touching the

element. The latter arrangement was found to give quicker and more stable control over cone temperature, and therefore, irradiance when specimen flames begin to impinge on the cone. The thermocouples should be of equal length and 0.16 to 0.32 mm diameter.

4.4 Hood System (Figures 15, 16)

The hood system is made from 24 gage stainless steel sheet for long life but does not need to be insulated because a heat balance is not made. A heavy-duty, cast iron, high temperature blower is required since temperatures up to about 340°C are obtained. The blower is equipped with a variable speed DC motor. At full speed flows in excess of 32 ℓ/s are possible. The normal operating point provides for a flow of about 24 ℓ/s. To provide proper mixing at the oxygen sampling probe, the duct inlet is provided with a 1/2 D entrance orifice (D = inside duct diameter). The ring probe is so located that at least 6 D of straight run upstream and 2 D downstream are available for flow straightening. The ring probe itself (Fig. 6) is welded into a flange which is then bolted between two flanges in the duct. This allows easy removal for inspection and cleaning. The hood system along with the blower and motor are mounted on rubber shock mounts to reduce the transfer of vibration to the rest of the apparatus.

Velocity measurement is made by use of a sharp-edged orifice plate located past the blower in the stack. The orifice is 1/2 D and is equipped with ASME "flange taps" [14] for measuring differential pressure. Pressure is measured with an electronic capacitative-type transducer. A thermocouple is located in the center of the duct, ahead of the orifice, for determining gas temperature and, thereby, density.

4.5 Specimen Mounting

(a) Horizontal Orientation (Figure 17)

Specimens are cut to 100 x 100 mm in size. Any thickness up to 50 mm can be accommodated. It is emphasized, however, that thermally thin specimens such as films, paints, etc., cannot be tested in any instrument in an

apparatus-independent way. These should be tested with the same substrate as will be used in their application. Adjustment for specimen thickness less than 50 mm may be made by inserting additional refractory pad layers. A spacing of 25 mm is maintained between the bottom of the cone and the top of the specimen. A minimum of 13 mm thickness of low-density (65 kg/m^3) refractory fiber pad is used inside the specimen holder underneath the specimen.

For rate of heat release testing specimen sides are protected with aluminum foil--a single piece is cut to fit on the bottom and sides and be cut flush with the top. This prevents spilling of any molten material and is sufficient in most cases to restrict burning along the edges. Composite specimens which involve a protective layer may have to be constructed by extending the protective layer down along the edges to envelop the more combustible layers within.

For ignitability testing there is sometimes the concern that the specimen should not ignite by localized heating at the edges. To prevent this, an outer frame (Fig. 18) is provided. This is placed on top of the specimen, which should nonetheless be wrapped with aluminum foil to facilitate cleaning. This frame weighs 415 g and can also serve to hold down any light specimens that need to be slightly compressed.

(b) Vertical Orientation (Figure 19)

In the vertical orientation, the same size specimens, 100 x 100 mm, are accommodated. If specimen thickness is less than 50 mm additional layers of refractory padding are used to fill out the depth and permit the spring clip to hold the specimen (Fig. 3). For 50 mm thick specimens a minimum of 13 mm millboard backing is used. The specimen sides and back are wrapped in aluminum foil. The vertical holder is provided with a small drip trough at the bottom to collect and retain molten residue. It is, however, inappropriate to test in the vertical orientation any materials which predominantly melt and drip.

No additional provision needs to be made for ignitability testing in the vertical orientation since the specimen holder is already equipped with a retaining edge around the front face.

4.6 Load Cell

A standard load cell is used having a live load capacity of 500 g. The particular instrument selected for use here has, additionally, a mechanical tare adjustment of 7 times its live load range. This feature allowed rugged, relatively heavy specimen holders to be designed without compromising mass loss resolution. The mechanical tare adjustment is set so that an empty specimen holder reads just barely on-scale.

The load cell is protected from heat by several techniques. Stainless steel spacer rods exposed to convective cooling are used as supports for the specimen holder plate (Fig. 20). A 13 mm layer of medium density (735 kg/m^3) refractory material is used as a spacer, and an additional layer of this same material is used as a radiation shield for the top of the cell (Fig. 4). Finally, in the horizontal orientation, where radiation to the cell is more severe, an operating technique is adopted of placing an empty specimen holder on the unit in between tests and during warm-up to serve as a shield.

The load cell electronics is equipped with a direct digital readout precise to 0.1 g.

4.7 Physical Adjustment of Apparatus

In the horizontal orientation the distance between the top of the specimen and the bottom of the cone can be adjusted in the test apparatus. In principle, raising the cone would decrease the available flux while increasing flux uniformity. In practice, it was found that the more serious effect is due to fire plume wander. To capture the combustion products within the confines of the cone it becomes advantageous to keep the cone as close as possible to the specimen. It was found that a spacing of about 25 mm gave the best results. To maintain this constant distance the heater position is adjusted when the specimen thickness is changed.

In the vertical orientation the cone position is adjusted so that the center of the cone corresponds to the center of the specimen.

Similarly, an adjustment can be made to the distance between the top of the specimen and the bottom of the exhaust hood. A large spacing can lead to a failure to capture some of the combustion products, while a small spacing can produce excessive impingement of the flames upon the exhaust duct. A suitable spacing is illustrated in figure 1.

4.8 Spark Ignition (Figures 21 and 22)

Earlier testing had indicated that use of spark ignition was preferable to a gas pilot since an electric spark does not impose a localized heat flux to the specimen surface and is easier to control and maintain. A commercial furnace-type spark plug is used which has 75 mm long electrodes and an approximately 27 mm insulator portion. This geometry permits the plug to be mounted outside the fire plume while the spark gap is located directly over the middle of the specimen. If a spark plug remains in the fire plume during the whole combustion period, it was seen that large soot streamers accumulated on the electrodes. Further, electrode life is reduced from prolonged heating. Thus, a sliding withdrawal mechanism was designed. The cone is equipped with two slotted brackets, one for horizontal and one for vertical orientation. The spark plug (Table 1) is mounted on a PTFE slide which is inserted into the appropriate bracket and lightly screwed down. The PTFE slide also retains a 10 kΩ series resistor, inserted in the HV line to minimize electromagnetic interference. The length of the bracket permits the spark plug to be fully withdrawn from the fire, using a handle, as illustrated in figures 2 and 3. The slide material was chosen to provide smooth travel, withstand elevated temperatures and provide electrical insulation. Chassis ground is not used, to minimize EMI. The spark power is supplied from a 10 kV transformer. Spark plug height is 13 mm above the center of a horizontal specimen and approximately 3 mm above the face plane of a vertical specimen. Two operating modes are possible--continuous spark and intermittent spark. The intermittent spark mode can be selected when a long time to ignition is expected.

4.9 Heat Flux Gage

A 12.5 mm diameter commercial Gardon gage of total heat flux type is used to measure flux to the specimen. The water-cooled gage is mounted in a square brass holder shown in figure 23. The holder fits into a square mounting collar welded to the edge of the cone bottom (Figs. 2, 3). The same mounting is used for both orientations. To change orientation the gage is merely inserted in the different orientation through the same square collar. The heights have been set so that gage face corresponds to the center of the specimen face plane in either orientation. The gage electrical output is read on a millivoltmeter and is not electrically grounded to chassis. The gage is removed prior to testing.

4.10 Calibration Burner (Figure 24)

A calibration burner was constructed to permit easy calibration between tests or as often as required. The burner is made of brass and has a square screened opening, packed below with refractory fibers. For use, it is inserted in the same square collar as is used for the heat flux gage. The burner orientation is chosen to discharge upwards, for either cone heater orientation. Typical operating calibration involves use of 99% pure methane at a flow corresponding to 10 kW.

5. ANALYSIS

5.1 Theory

The equations necessary to implement a practical realization of the oxygen consumption principle have been presented by Parker [15]. From the basic theoretical relationship

$$\dot{q} = \left(\frac{\Delta h_c}{r_o}\right)\left(\dot{m}_{O_2,\infty} - \dot{m}_{O_2}\right)$$

an operating equation must be evolved. While it is not feasible to measure oxygen mass-flow, oxygen volume-fraction is readily determinable. Furthermore, depleted oxygen measurements must, perforce, be made on the

exhaust stream. Since the mass flow in the exhaust stream is different from the mass flow in the intake air stream by the amount of the gasified fuel mass, an adjustment is needed, based on stoichiometry. Finally, with most O_2 analyzers, water has to be trapped out of the sample stream. For simpler analysis, it is also convenient to trap out CO_2. Then from [15] it is seen that

$$\dot{q} = \left(\frac{\Delta h_c}{r}\right) \frac{M_{O_2}}{M_{air}} \dot{m}_e \frac{\left(X^o_{O_2} - X_{O_2}\right)}{\left[1 + (b - 1)X^o_{O_2}\right] - bX_{O_2}}$$

where the denominator accounts for the difference in exhaust/intake mass flows. Also included is the assumption that CO, HCℓ, and other possible minor combustion products are volumetrically negligible. Some typical values include:

Fuel	b	$\left[1 + (b - 1)X^o_{O_2}\right]$	$\frac{\Delta h_c}{r_o}$ (kJ/kg)
Methane (CH_4)	1.5	1.105	12.54×10^3
Propane (C_3H_8)	1.4	1.084	12.78×10^3
Ethylene (C_2H_4)	1.33	1.070	13.78×10^3
PMMA ($nC_5H_8O_2$)	1.5	1.105	12.97×10^3

setting $X^o_{O_2} = 0.2095$ and $b = 1.5$ gives

$$\dot{q} = \left(\frac{\Delta h_c}{r_o}\right) \frac{32}{28.97} \dot{m}_e \frac{\left[0.2095 - X_{O_2}\right]}{\left[1.105 - 1.5\ X_{O_2}\right]}$$

Huggett [9] recommends taking $\Delta h_c/r_o = 13.1 \times 10^3$ for arbitrary fuels; he also tabulated specific values for a variety of fuels. Additional values are available in [16]. It can be seen for most common fuels $\Delta h_c/r_o$ is within 5% of 13.1×10^3. Thus, in computations the value of $\Delta h_c/r_o$ is set to 13.1×10^3 for unknown fuels, to 12.54×10^3 for the calibration methane gas, and to its actual value if the test material composition is known.

The mass flow rate through the system, $\dot{m}_e$, can be computed from the orifice meter pressure drop and the temperature as

$$\dot{m}_e = C\sqrt{\frac{\Delta P}{T_e}}$$

Then

$$\dot{q} = (13.1 \times 10^3)(1.10)\, C\sqrt{\frac{\Delta P}{T_e}}\, \frac{\left[0.2095 - X_{O_2}\right]}{\left[1.105 - 1.5\, X_{O_2}\right]}$$

and the rate of heat release per unit area is

$$\dot{q}'' = \dot{q}/A_s$$

If a CO_2 analyzer is available then trapping of CO_2 is not necessary. The rate of heat release expression, however, becomes more complex since CO_2 terms must be included,

$$\dot{q} = \left(\frac{\Delta h_c}{r_o}\right)\frac{32}{28.97}\,\dot{m}_e\,\frac{1}{\dfrac{1 - X_{O_2} - X_{CO_2}}{X^o_{O_2}\left(1 - X_{CO_2}\right) - X_{O_2}\left(1 - X^o_{CO_2}\right)} + (b - 1)}$$

The equations above can be used directly by measuring the various required variables. In practice, as is discussed in section 8.5.1, the value of C is difficult to determine directly to better than ± 5%. Also, the value of $X^o_{O_2}$ may not be exactly 0.2095, as assumed. Both of these potential sources of error are eliminated if the apparatus is, instead, calibrated with a known fixed methane burner flow and an effective C value computed from that.

5.2 Analysis of Data

5.2.1 Manual Analysis

Manual analysis of the data is possible. This is tedious for any but the shortest tests. In applying the equation all the measurements should be at a consistent time. Temperature and pressure readings are nearly instantaneous. Oxygen readings, however, are subject to a large delay due to transit time through pipes and traps (see section 8.4). Thus oxygen data have to be offset with respect to the others to obtain proper results.

5.2.2 Electric Analog Signal Conditioning

It is possible to build an analog signal module to perform appropriate mathematical operations: multiplication, division, subtraction, and square roots. A circuit diagram for such a device is shown in figure 25. For a rigorous application of the equation, however, the oxygen signal would have to be delayed with respect to the others. No simple, practical device is readily available that could do this for the long delay times required. Without such a delay, an error is introduced which is proportional to the rate of change of $\dot{q}$ with time. Thus an analog device of this nature is limited in usefulness to fairly steady heat release conditions.

5.2.3 Digital Data Collection

Most of the data were gathered on a digital data collection and reduction system. Such a method can provide needed delay times of arbitrary length. This arrangement also readily permits specimen mass loss rates to be computed and an effective heat of combustion to be obtained as

$$\Delta h_{c,eff} = \dot{q}/\dot{m}_p$$

The operation of the system in general terms is as follows. Details are available in [17]. Data collection and analysis are done in separate passes. In the data collection phase the following data channels are set up to be scanned: real-time clock, oxygen concentration, ΔP, stack temperature, load cell, and, optionally, CO_2 and CO. A floppy disk is inserted and the starting address selected. The data collection program first asks for test title and heading. Next, either a single scan is recorded of values during a 10 kW gas burner burn, or else the previous calibration constant is entered. The scan interval is set next (3 s for shorter tests, 6 s for longer). Scanning is now started at regular intervals when the start button is pressed. After the test is completed a final end-of-test trailer is written on the disk and the procedure can be re-initiated for the next test.

In the data analysis phase, the proper test data are first read in from the floppy disk into memory. The time channel is checked for consistency and

real-time values converted to test time. At this point also an optional value of $\Delta h_c/r_o$ other than the standard one may be entered. Next, the gas analyzer data are all time-shifted by the delay time value (see section 8.4). Heat release rate values are next determined and $\dot{q}''$ computed. These computations are started after the last negative $\dot{q}''$ value (small noise component) is passed. Also computed is the running total

$$q'' = \sum_i \dot{q}_i'' \, \Delta t$$

Next the mass loss curve is examined for outliers; the $\dot{m}_p$ curve is obtained by making a least squares fit of a slope to the mass curve, taken over 10 points each side of the desired one. The heat of combustion is then computed over a running 15 s time-base. This curve is again slightly smoothed by the use of a 3-point average. Air flow rate and CO_2 and CO concentrations are simply determined from the appropriate input readings. Output is available in three forms. (1) Tabular output of $\dot{q}''$, $\dot{m}''$, Δh_c, $\dot{m}_e$ and CO_2 and CO, at appropriate time intervals. (2) Plots of $\dot{q}''$, Δh_c or other variables of interest. (3) Tape file output of reduced data, to be used for further plotting or analysis.

6. TEST PROCEDURE

Initially, the following calibrations were performed: the oxygen meter response time setting was adjusted (not all oxygen meters have this control). This control was adjusted by using the calibration burner and observing the response when the gas flow is abruptly shut off. The response speed was increased until an O_2 response undershoot was just barely observed. Next, the heater temperature controller was calibrated against Gardon gage readings, separately for the two orientations. Finally, a 10 kW CH_4 flow calibration was performed.

During routine testing the following procedure was used. The thermoelectric trap was turned on about 30 minutes before test time. Any accumulated water was drained out of the separation chamber. The drying and CO_2 removal traps were checked and replaced if needed. A new soot filter was inserted. The oxygen meter was spanned using room air and zeroed using N_2.

An orientation was selected and the cone set for that orientation. For horizontal specimens the height was set to be appropriate for specimen thickness. The heater was turned on and set to a control temperature corresponding to the desired flux. For horizontal testing, a blank specimen holder was placed on the holder plate. The exhaust blower was turned on. After the control temperature was reached, a further 5 minutes was allowed for full equilibration. The ignition spark plug was checked for condition and cleaned if dirty. The load cell zero control was adjusted. The sample gas pump was started.

The data collection system was initialized. Calibration values for 10 kW CH_4 flow were measured, if not previously done on that day. The specimen, wrapped in aluminum foil, was placed in a cold holder. The empty holder was removed (horizontal only) and the specimen in its holder placed on the holder plate. The data collection system was started. The last two operations could be performed in well under 2 s. The spark plug holder was pushed in. Sparking was started immediately for unknown specimens. With specimens whose ignition times are roughly known, however, start of spark could be appropriately delayed. Upon ignition, the spark plug was withdrawn. For ignitability testing the time to ignition was determined with a stopwatch to 0.2 s. Otherwise, a record of ignition time was available on the data collection system, with a resolution of 1 scan (normally 3 s). After flaming ceased, the specimen holder was removed. For horizontal testing the foil and residue were discarded and the empty holder returned to position. If a specimen did not ignite within 10 minutes, it was also removed and discarded.

7. TEST LIMITATIONS

In addition to requirements for specimen size and shape, the following limitations emerged:

1) The specimen must not swell sufficiently to interfere with spark plug operation or with the heater. This effectively limits swelling to 10 mm for horizontal specimens and 20 mm for vertical ones. The use of the ignitability frame for horizontal specimens may be beneficial in limiting swelling.

2) Specimens must not show explosive spalling or delamination. When this occurs ignitability is difficult to determine and the concept of a rate of heat release per unit area becomes dubious.

3) Any amount of melting can be tolerated for horizontal specimens, including even liquid specimens. For the vertical orientation, however, only very limited melting can be acceptable, i.e., only what can be contained in the melt trough. It should be noted that with some materials melting tendency is highly dependent on the irradiance.

8. PERFORMANCE

8.1 General Observations

One general requirement is that the hood system be able to collect all of the combustion products. This can be visually verified--no spillage over the side nor flow back-up is observed. Cross-draft conditions may result in a significant amount of plume wander. While an environmental enclosure, per se, is not required, it is appropriate to only operate in laboratory spaces without significant drafts or pressure fluctuations.

For realistic representation of the burning process, the apparatus should not distort the pool-plume or wall-plume which would be exhibited by a free-burning specimen. In the horizontal configuration the cone heater is quite close to the fire plume. Yet observations under a wide range of conditions do not show any significant deflection of plume streamlines. The plume can pass out the cone top opening since it naturally necks down above the base. Further, fresh air is entrained alongside the plume; thus the stream flowing by the heater element has an outer layer of cooler air. Since the plume does show turbulence, occasionally small flame packets will impinge upon the cone top plate or bottom plate. These do not represent a significant portion of the total flow.

8.2 Exhaust System

For the orifice plate used, a relation was derived from formulas given in [14] as

$$\dot{m}_e = C\sqrt{\frac{\Delta P}{T_e}}$$

where C is a constant in the vicinity of 0.03, ΔP is measured in Pascals and T_e in Kelvins. For an orifice to the exact ASME specifications, $C \simeq 0.031$. The orifice plate installation used does not fully conform to the intent of the ASME calibrations, because sufficient flow straightening would be difficult to provide in the available space. As a result, a calibration was made by using CO_2 as a tracer gas. Under cold conditions CO_2 was metered into the hood from a bottled supply. Gas readings were taken using the existing gas instrumentation. The calibration showed $C = 0.028$ with an uncertainty of $\pm$ 5%. This is the value that is then used in checking the relative instrument calibration results. It is further expected that this value can change slightly with time as soot builds up on the orifice edge. The instrument accuracy will not, however, change due to that since the operating calibration procedure (section 6) takes into account any change in the value of C.

The relationship between mass and volume flows was explored at two temperature conditions (ambient and $\dot{Q}$ = 10 kW) and at 6 flow settings (table 2). This shows that, as expected for fans in general, volume flow rates remain nearly constant, even when temperatures and mass flows vary substantially. It is also interesting to compute $\dot{Q}_{conv}$, the convective heat flow. Only 20 to 41% of the total heat released was seen to be collected as convective duct flow. The rest is radiated out directly from the fire plume, radiated from the exhaust system and convected away from the duct exterior. Since this is an oxygen-consumption instrument, no effort needs to be made to increase this fraction.

For optimum response with a minimum of noise, the time constants on the pressure transducer and stack thermocouple have to be adjusted to be slightly faster than the O_2 meter. Time constants of 1 to 3 s were considered appropriate. A stack temperature traverse is indicated in table 3.

8.3 Cone Heater

Table 4 shows the relationship between heater temperatures and measured fluxes to a specimen. It is noteworthy that horizontal and vertical calibrations are nearly identical, showing the limited role of convective fluxes. A view factor, F, as such cannot be computed from basic geometry since the cone edges do not drop abruptly from uniformly high temperature to ambient, although if such a simplification is made, F = 0.79 is computed. It is readily possible, however, to compute

$$\varepsilon F = \frac{\dot{q}''_g}{\sigma\left(T_h^4 - T_\infty^4\right)}$$

The values in table 4 show this combined emissivity view factor product to be around 0.85, which includes also the convective contribution. The emissivity will vary slowly with time due to changes in the heater surface condition, thus necessitating periodic calibration. Table 5 shows additional calculations of the convective flux component, computed from measurements with two Gardon gages, one of which had a window to eliminate convective heating. In the horizontal orientation the convective flux is negligibly small, but in the vertical orientation small values, only mildly dependent on the total flux, may be measured.

Incident flux uniformity is indicated in table 6. Measurements were taken with a small Gardon gage on a nine-point grid (32 mm spacing). In the horizontal orientation peak deviations are typically ± 2%. In the vertical orientations the deviations vary according to flux level. While the radiative component is roughly constant, the convective flux increases towards the top. Under all conditions, the center flux is nearly identical to the average flux, although for more precise computation, it can be taken as 1.02 times the average.

8.4 Oxygen Analyzer Response

The measuring system does not respond instantaneously to oxygen level changes due to two separate causes. (1) A finite time is required to move the sample through the lines, traps, pump, and into the oxygen analyzer; and

(2) the oxygen analyzer itself does not respond instantaneously. Several adjustments are available that affect the response time. The gas sampling train (Fig. 7) uses a bypass waste arrangement with an adjustable bypass relief pressure. This was set so that 0.25 ℓ/min flows through the oxygen analyzer, 0.75 ℓ/min flows through the (optional) CO_2 and CO analyzers, while 3.3 ℓ/min is bypassed. The absolute back-pressure regulator was set for 1.05 standard atmospheres which is substantially higher than recorded barometric highs in our location.

Another adjustment is an electrical O_2 analyzer response time setting, available on the make of analyzer used here. This can be adjusted to its optimum value by establishing a steady burner fire and then abruptly shutting off the gas flow. The oxygen response control is speeded up until a barely perceptible overshoot is obtained during return to baseline.

It was found that the oxygen response to a unit step input could be described as

$$s(t) = 1 - e^{-\beta(t - t_d)} \qquad t - t_d > 0$$
$$= 0 \qquad t - t_d \leq 0$$

Here t_d is the transit delay time and β is the time constant for the O_2 analyzer. The constants found were t_d = 30 s and $\beta = 0.32\ s^{-1}$. These values were determined upon shutting burner flow off. Turn-on behavior cannot be measured as readily since a pressure surge is difficult to avoid at ignition. The constants did not vary with $\dot{q}$.

8.5 Calibrations with Pure Gases

To be assured of correct operation, the apparatus must show linearity when presented with calibration gases over a wide range of flows. Also, the determination of the heat release rate should not be dependent on the relative radiance of the flames or on stoichiometric requirements. Methane was chosen for all the basic calibrations, supplemented by propane and ethylene as suitably different gases (section 8.5.2). Table 7 shows the linearity and noise over a range of 1 - 12 kW. The measured response was determined ten

different times for each flow rate using the data acquisition/reduction routines. The linearity is within 5% over the entire range and within 2% over 5 to 12 kW. The noise is at about ± 2% throughout.

The burner used (Fig. 24) necessarily has a fixed height and fixed throat size. It was desired to determine whether burner size and location have a significant effect. For this purpose an additional burner was constructed with an opening of 100 x 100 mm. Measurements were made at nine different heights. Table 8 shows that there is no detectable influence of burner height, except when extremely close to the hood. The average difference in response between the standard burner and the large burner is 3%.

The blower speed and the exhaust flow rate would be expected to have some effect on instrument performance. At very slow speeds it would be expected that incomplete combustion product collection would result, while at excessively high speeds the change in oxygen concentration would be too small for adequate resolution. Table 9 shows the results of measurements at two different heat release levels, corresponding to slow burning and fast burning specimens. Flows were varied over the total range available. The results show a very shallow minimum for noise around 0.018 to 0.024 m^3/s. The conclusion, however, is that noise does not indicate the selection of a specific exhaust flow: less than ± 2% noise can be obtained at any available flow rate.

8.5.1 Oxygen/Carbon Dioxide Balance

One available check on the performance of the instrument is the O_2/CO_2 balance. For complete combustion of a given fuel there is a fixed ratio of oxygen consumed to carbon dioxide generated. For example, for methane

$$CH_4 + 2O_2 \rightarrow CO_2 + 2H_2O$$

In other words, for each mole of CO_2 generated there should be two moles of O_2 consumed

$$\frac{n^o_{O_2} - n_{O_2}}{n_{CO_2}} = 2.$$

where n denotes molar flows. The ratio is determinable from measured quantities X_{O_2} and X_{CO_2} as

$$\frac{n^o_{O_2} - n_{O_2}}{n_{CO_2}} = \frac{\left(X^o_{O_2} - X_{O_2}\right)\left(1 - X_{CO_2}\right)}{X_{CO_2} \quad \left(1 - X^o_{O_2}\right)}$$

The CO_2 readings here refer to adjusted values, with the small ambient concentration (~0.04%) subtracted out. Also, the O_2 readings here refer to a sample line where CO_2 (and H_2O) has been scrubbed out. Table 10 shows the results of these calibrations. The calculated values are quite close to the expected 2.0 value.

The ratio of measured to supplied $\dot{q}$ values here refers not to a relative gas burner calibration, but rather to a value calculated from using the mass flow calibration as C = 0.028. The close agreement, to within less than 3% difference, of the measured and the supplied values verifies that the tracer gas method agrees well with the individual combustion calibrations.

In the same vein, calculations can be made of the absolute flows of O_2 and CO_2. At a given flow of methane

$$\dot{m}_f = \dot{Q}/\Delta h_c$$

Also, from stoichiometry, for complete combustion

$$\dot{m}_{CO_2} = (\dot{m}_e - \dot{m}_f)\,\frac{44}{28.97}\,\frac{\left(1 - X^o_{O_2}\right) X_{CO_2}}{\left(1 - X_{O_2}\right)\left(1 - X_{CO_2}\right)}$$

is the flow of CO_2 in the exhaust, based on measured $\dot{m}_e$ and gas analyzer readings. Similarly, the change in oxygen flow in the exhaust is

$$\dot{m}_{\Delta O_2} = (\dot{m}_e - \dot{m}_f)\,\frac{32}{28.97}\,\frac{\left(X^o_{O_2} - X_{O_2}\right)}{\left(1 - X_{O_2}\right)}$$

The expected flows, meanwhile, are

$$\dot{m}_{CO_2} = \frac{44}{16}\,\dot{m}_f = 2.75\,\dot{m}_f$$

$$\dot{m}_{\Delta O_2} = \frac{64}{16} \dot{m}_f = 4 \dot{m}_f$$

The data in table 10 verify that the measured value of C = 0.028 is to within about 2% of the correct value.

From the above findings it can be seen that the absolute calibration has about a 5% uncertainty. Comparison with the data in table 7 indicates, however, that linearity to within 2% over a large portion of the range is obtainable when a gas burner supplying methane at a $\dot{q}$ = 10 kW level is used. Thus, for operational purposes the gas burner calibration is to be preferred.

8.5.2 Other Gases

For a heat release apparatus to be satisfactory, the proper heat release should be measured for any fuel. For gases, two additional fuels were chosen, intended to exemplify gases more prone to sooting--propane and ethylene. Table 11 shows the results. An average recovery of 1.00 for propane and 0.97 for ethylene is seen. It is reasonable to suppose that for ethylene the bulk of the 3% not recovered goes to soot.

8.6 Heat Release Measurements on Solid Materials

Illustrative measurements are shown on two materials: black polymethylmethacrylate (PMMA) and red oak. PMMA was chosen as exemplifying a thermoplastic material with minimum tendency to drip, while the red oak is characteristic of woods and char-forming materials in general. The red oak had a density of 778 kg/m^3, conditioned at 50% R.H. and 23^{o}C while the PMMA had a density of 1184 kg/m^3. Test thicknesses were 20 mm for red oak and 25 mm for PMMA. The PMMA used was black in order to minimize diathermanous heating effects.

Data for rate of heat release and effective heat of combustion under an irradiance of 50 kW/m^2 are shown in figures 26 and 27. For PMMA the effective heat of combustion should be constant. The data show this constancy except at the start and the end where the $\dot{m}$ values change very fast. Under those conditions an instantaneous Δh_c is not readily computable. The average Δh_c

obtained from sixteen tests is (24.2 ± 1.1) x 10^3 kJ/kg. The effective net heat of combustion fraction is 24.2/24.88 = 0.97. For red oak a constant heat of combustion is not expected since there is not a unique degradation mechanism. During steady burning $\Delta h_c \approx 10 \times 10^3$ kJ/kg, but there is a peak at the start of about 12 x 10^3 kJ/kg and second peak near the end 15 x 10^3 kJ/kg. Negligible PMMA weight remains at the end of the test, while up to 20% of the red oak mass remains when the fire goes out.

Figures 28 and 29 show the heat release rates under different irradiance conditions, 25, 50, and 75 kW/m^2. Horizontal PMMA measurements (Fig. 28) show a pre-ignition period, then a rapid rise, followed by slower equilibration to nearly a steady state. Towards the end of the test the heat wave reaches the back face and the burning rate increases. Just prior to burnout there is usually a rapid increase in $\dot{q}$". This can be physically seen to be due to formation of globules--the material burns over an effective area greater than the 100 x 100 mm projected area. Comparison of horizontal and vertical conditions shows a significantly higher burning rate at the horizontal orientation, amounting to about 80 kW/m^2. This is not unexpected since the heat flux to the fuel from the flames themselves is much higher in the horizontal configuration than in the vertical.

The red oak specimens show a very different behavior (Figs. 30 and 31). The horizontal $\dot{q}$" values are again higher than the vertical. The second peak arises because the specimen at that point is heated through to the rear face and no longer behaves as if thermally thick. The bulk of the heat is released during this later heating, after the first peak is passed. At the end of such a test it can be observed that the original volume of the sample is almost maintained in the form of the char structure, but that the weight associated with it is very small.

Test repeatability with solid materials burning is somewhat harder to assess than with gases. Resolution with gases is limited due to turbulence in the burning plume itself and due to noise in the measuring instrumentation. With solids, however, a third factor is introduced, namely variability in the pyrolysis rate. Real solids, even if subjected to uniform external heating and flow fields, pyrolyze somewhat randomly and burn non-uniformly. Indeed,

one can sometimes see solid or molten particles being ejected out away from the surface. Thus, there is a certain limit to the measurement precision due to burning behavior irregularities. To illustrate the response, however, figure 32 shows three tests on 25 mm PMMA samples heated at 25 kW/m^2. To assess repeatability numerically, it is most appropriate to consider the total heat released during the entire combustion. When normalized by the specimen mass this becomes simply the time-average heat of combustion. The figure cited above is $24.2 \pm 1.1 \times 10^3$ kJ/kg, or a variation of ± 5%.

9. CONCLUSIONS

A bench-scale apparatus has been developed for measuring rates of heat release of flat materials by use of the oxygen consumption principle. The exclusive use of the oxygen consumption principle has allowed an efficient, rugged, accurate instrument to be designed which is neither physically large nor expensive to construct. The instrument shows a linearity generally to within 5% and over the major operating region to within 2%. Noise is also within 2%. Fuels of known combustion characteristics show recovery of known heat of combustion to within the noise level of the apparatus. Proper control of external heating, a problem with some heat release rate apparatuses has been designed into the fundamental geometry. Mass loss and effective heat of combustion measurements have been incorporated as part of the operation.

10. ACKNOWLEDGMENTS

David Swanson prepared shop drawings and constructed major portions of the apparatus. Robin Breese conducted tests necessary for the development of the apparatus. William Parker collaborated in the project at several stages. Emil Braun wrote the data collection and analysis routines. The Consumer Product Safety Commission provided partial support through its Plastics Flammability Research Project.

11. REFERENCES

[1] V. Babrauskas, et al., Upholstered Furniture Heat Release Rates Measured with a Furniture Calorimeter, Nat. Bur. Stand. (U.S.), NBSIR 82-(1982).

[2] V. Babrauskas, Combustion of Mattresses Exposed to Flaming Ignition Sources, Part II. Bench-Scale Tests and Recommended Standard Test, Nat. Bur. Stand. (U.S.), NBSIR 80-2186 (1981).

[3] N. J. Thompson, E. W. Cousins, The FM Construction Materials Calorimeter. NFPA Q. 52, 186-192 (Jan. 1959).

[4] W. J. Parker, M. E. Long, Development of a Heat Release Rate Calorimeter at NBS, pp. 135-151 in Ignition, Heat Release and Noncombustibility of Materials (STP 502). American Society for Testing and Materials, Philadelphia (1972).

[5] J. P. Tordella, W. H. Twilley, Development of a Calorimeter for Simultaneously Measuring Heat and Mass Loss, Nat. Bur. Stand. (U.S.), to be published.

[6] J. R. Lawson, private communication.

[7] Proposed Test Method for Heat and Visible Smoke Release Rates for Materials. American Society for Testing and Materials, Annual Book of Standards, Part 18 (1981).

[8] V. Babrauskas, Performance of the OSU Rate of Heat Release Apparatus Using PMMA and Gaseous Fuels, Fire Safety J. 5, 9-20(1982).

[9] C. Huggett, Estimation of Rate of Heat Release by Means of Oxygen Consumption Measurements. Fire and Materials. 4, 61-65 (1980).

[10] G. Svensson, B. Östman, Rate of Heat Release for Building Materials by Oxygen Consumption. STFI Meddelande Serie A, nr. 761 (May 1982).

[11] G. S. Holmstedt, Rate of Heat Release Measurements with the Swedish Box Test (SP-RAPP 1981:30). Statens Provningsanstalt, Boras, Sweden (1981).

[12] D. Bluhme, Nordtest Project 115-77, Part 2: ISO RHR Test Apparatus with Oxygen Consumption Technique, Dansk Institut for Prøvning og Justering, Copenhagen (1982).

[13] Technical report ISO/TR 5657-1982 (E), Fire Test-Reaction to Fire - Ignitability of Building Materials, International Organization for Standardization (July 1982).

[14] Fluid Meters, Their Theory and Application. Report of ASME Research Committee on Fluid Meters. American Society of Mechanical Engineers, New York (1971).

[15] W. J. Parker, Calculations of the Heat Release Rate by Oxygen Consumption for Various Applications, Nat. Bur. Stand. (U.S.), NBSIR 81-2427 (1982).

[16] Fire Protection Handbook, tables in Chapter 4. National Fire Protection Association, Quincy, MA (1981).

[17] Data Collection and Analysis Programs, written for Tektronix 4052. Copy available from author.

[18] D. L. Sensenig, An Oxygen Consumption Technique for Determining the Contribution of Interior Wall Finishes to Room Fires, Nat. Bur. Stand. (U.S.), Tech. Note 1128 (1980).

Table 1. List of Major Parts*

Mechanical

Heater element -- Welman Co. "Calrod" TY 3272 (8 mm dia., 3.38 m long 5000 W, 240 V max)
Temperature controller -- Barber Colman 5624-12-035-330-0-00
Power controller -- Robicon 313-223
Fan -- Westinghouse cast iron, high temperature type, model 504 (BAY9657-1)
Variable speed motor with controller (3/4 HP) -- Dayton 2Z846
Heat flux gauge -- Medtherm Co. GTW-7-32-485A
Pressure transducer - MKS Instruments 223AH-A-10
Spark plug -- Eclipse Combustion 12568
Ignition transformer -- Dongan A10-LA2
Load cell -- Automatic Timing and Controls 6005C06EIXX (with external demodulator)

Oxygen Sampling

Soot filter -- Nuclepore 490605 (support only)
Pump -- Thomas Industries 908CA18
Waste regulator -- Norgren V06-221-NNAA
Supplemental drier -- W. A. Hammond Co. "Drierite"
CO_2 removal media -- A. H. Thomas Co. "Ascarite"
Flow regulator -- Moore 63BDL
Final filter -- Nupro SS-4FW-7
Oxygen analyzer -- Beckman 755 (0-25% range)
Absolute back pressure regulator -- Moore 43R
Thermoelectric cooling modules -- Cambion Thermionic 806-1001-01

*Certain commercial equipment, instruments, and materials are identified in this publication in order to adequately specify the experimental procedure. Such identification does not imply recommendation or endorsement by the National Bureau of Standards, nor does it imply that the materials or equipment identified are necessarily the best for the purpose.

Table 2

Exhaust System Flows

Fan Setting (Arbitrary)	$\dot{Q}$ = 0			$\dot{Q}$ = 10 kW CH_4				
	ΔP (Pa)	$\dot{V}_e$ (m^3/s)	$\dot{m}_e$ (kg/s)	T (K)	ΔP (Pa)	$\dot{V}_e$ (m^3/s)	$\dot{m}_e$ (kg/s)	Q_{conv} (kW)
50	90	0.0146	0.0173	503	48	0.0138	0.0097	2.00
60	156	0.0193	0.0229	498	80	0.0178	0.0126	2.53
70	241	0.0239	0.0284	496	124	0.0222	0.0158	3.14
80	334	0.0282	0.0335	481	194	0.0274	0.0201	3.70
90	428	0.0319	0.0379	453	249	0.0300	0.0234	3.65
100	448	0.0327	0.0388	468	274	0.0320	0.0241	4.12

T_∞ = 297 K

$\dot{Q}_{conv} = 1.0\ (T - T_\infty)\dot{m}_e$

Table 3

Stack temperature map

Fraction of radius	Temperature rise (K)
0. (center)	155
0.1	155
0.2	156
0.3	156
0.4	156
0.5	156
0.6	155
0.7	150
0.8	148
0.9	117
1.0 (edge)	86

Exhaust flow = 0.023 m^3/s

Methane supply = 5 kW equivalent

Table 4

Radiation from Cone Heater

Horizontal				Vertical		
Irradiance $\dot{q}''_g$ (kW/m^2)	Heater Temp. (^oC)	$\sigma(T_h^4-T_\infty^4)$ (kW/m^2)	εF (--)	Heater Temp. (^oC)	$\sigma(T_h^4-T_\infty^4)$ (kW/m^2)	εF (--)
10	422	12.8	0.78	424	12.9	0.77
20	547	25.2	0.79	546	25.1	0.79
25	592	31.3	0.80	590	31.0	0.81
30	628	37.0	0.81	626	36.6	0.82
40	689	48.1	0.83	689	48.1	0.83
50	744	60.2	0.83	742	59.7	0.84
60	783	70.0	0.86	786	70.9	0.85
70	825	82.0	0.85	825	82.0	0.85
75	841	86.9	0.86	843	87.5	0.86
80	860	93.0	0.86	861	93.3	0.86
90	892	104.0	0.87	890	103.3	0.87
100	919	114.0	0.88	918	113.6	0.88
110	943	123.5	0.89	946	124.8	0.88

Table 5

Effect of Convective Fluxes

Horizontal Orientation

No observable difference from 20 to 110 kW/m^2 (± 3%)

Vertical Orientation

Measured fluxes (kW/m^2)		
Total	Radiant	Convective (By Difference)
10.0	8.1	1.9
20.0	17.6	2.4
29.9	26.7	3.2
40.0	34.7	5.3
49.7	43.8	5.9
59.8	54.9	4.9
70.2	64.7	5.5
80.0	72.2	7.8
90.0	82.7	7.3
100.2	91.8	8.4
110.5	102.6	7.9

Table 6

Flux Deviation Summary

Nine-point grid, spacing at 32 mm

Orientation	Irradiance (kW/m^2)	Ratio $\frac{\text{center}}{\text{average}}$	Peak deviations from avg.
horizontal	25	1.01	-2%, +1%
	50	1.03	-2%, +1%
	75	1.00	-3%, +2%
vertical	25	1.02	-11%, +8%
	50	1.02	-8%, +7%
	75	1.03	-6%, +4%

Table 7

Linearity of Response

CH_4 supply rate[1] (kW)	Measured response[2] (kW)	Fraction	Noise
0.98	0.94	0.96	±2.4%
2.01	1.82	0.95	±1.7%
2.99	2.94	0.98	±1.9%
3.95	3.77	0.95	±2.6%
4.99	5.01	1.00	±0.5%
5.97	5.88	0.98	±1.1%
6.94	6.89	0.99	±1.1%
8.04	7.89	0.98	±1.7%
8.96	8.76	0.98	±0.7%
9.93	9.93	1.00	±2.0%
10.93	10.68	0.98	±1.4%
11.94	11.66	0.98	±1.0%

Exhaust flow = 0.022 m^3/s

(1) Calculated using net heat of combustion of 50.0 MJ/kg

(2) With apparatus calibrated at 10 kW

Table 8

Burner Height Effect for 10 kW Methane Flow

Burner head distance below lip of hood (mm)	Calculated Heat Release Rate (kW)		Ratio
	Standard burner	100 x 100 mm burner	
12	9.75	10.18	1.012
38	9.87	10.29	1.043
64	10.05	10.30	1.025
89	10.08	10.40	1.032
114	10.12	10.39	1.027
140	10.05	10.41	1.036
165	10.06	10.36	1.030
191	10.13	10.42	1.029
216	10.09	10.34	1.025

Table 9

Effect of Air Flow Rate on Noise

Methane Supply (kW)	Fan Setting (Arbitrary)	$\dot{V}$ (m^3/s)	Measured $\dot{Q}$ (kW)
2	50	0.015	2.00 ± 0.04
2	60	0.019	1.98 ± 0.02
2	70	0.024	1.98 ± 0.008
2	80	0.028	2.00 ± 0.03
2	90	0.032	1.99 ± 0.02
2	100	0.033	1.97 ± 0.01
10	50	0.014	9.86 ± 0.14
10	60	0.018	9.82 ± 0.08
10	70	0.022	10.00 ± 0.17
10	80	0.027	10.14 ± 0.14
10	90	0.030	10.13 ± 0.15
10	100	0.032	10.14 ± 0.19

Table 10

Oxygen/Carbon Dioxide Balance

Test	T (K)	ΔP (Pa)	$\dot{m}_e$ (kg/s)	O_2 (%)	$\dot{Q}_{supplied}$ (kW)	$\dot{Q}_{meas}$ (kW)	$\frac{\dot{Q}_{meas}}{\dot{Q}_{suppl}}$	CO_2^* (%)	$\left(\frac{n^o_{O_2} - n_{O_2}}{n_{CO_2}}\right)$
0	---	---	--	20.93	0	0	--	0	--
1	377	220	0.0214	20.43	1.84	1.86	1.01	0.30	2.10
2	437	184	0.0182	19.76	3.56	3.64	1.02	0.69	2.13
3	525	144	0.0147	18.41	6.10	6.19	1.01	1.42	2.22
4	586	124	0.0129	16.98	8.22	8.30	1.01	2.23	2.19
5	578	113	0.0124	15.79	10.25	10.16	0.99	3.18	1.98
6	651	101	0.0110	13.50	12.13	12.54	1.03	4.42	2.03

Test	Supply $\dot{m}_f$ (g/s)	Expected $\dot{m}_{CO_2}$ (g/s)	Expected $\dot{m}_{\Delta O_2}$ (g/s)	Measured $\dot{m}_{CO_2}$ (g/s)	Measured $\dot{m}_{\Delta O_2}$ (g/s)	$\frac{\text{Meas.}}{\text{Expected}}$ CO_2	$\frac{\text{Meas.}}{\text{Expected}}$ ΔO_2
1	0.037	0.102	0.148	0.097	0.148	0.95	1.00
2	0.072	0.198	0.288	0.189	0.292	0.95	1.01
3	0.122	0.336	0.488	0.309	0.497	0.92	1.02
4	0.164	0.451	0.656	0.420	0.669	0.93	1.02
5	0.205	0.564	0.820	0.571	0.822	1.01	1.00
6	0.243	0.668	0.972	0.691	1.02	1.03	1.05

*Baseline values subtracted out.

Table 11

Rate of Heat Release for Additional Gases

Propane ($\Delta h_c/r_o$ = 12.78 x 10^3 kJ/kg)

Supplied (kW)	Measured (kW)	Meas./Suppl.
3.13	3.20	1.02
5.43	5.50	1.01
6.96	6.95	1.00
8.7	8.8	1.01
10.2	10.1	0.99

Ethylene ($\Delta h_c/r_o$ = 13.78 x 10^3 kJ/kg)

Supplied (kW)	Measured (kW)	Meas./Suppl.
3.38	3.30	0.98
5.97	5.75	0.96
7.83	7.55	0.96
9.4	9.2	0.98
11.8	11.5	0.97

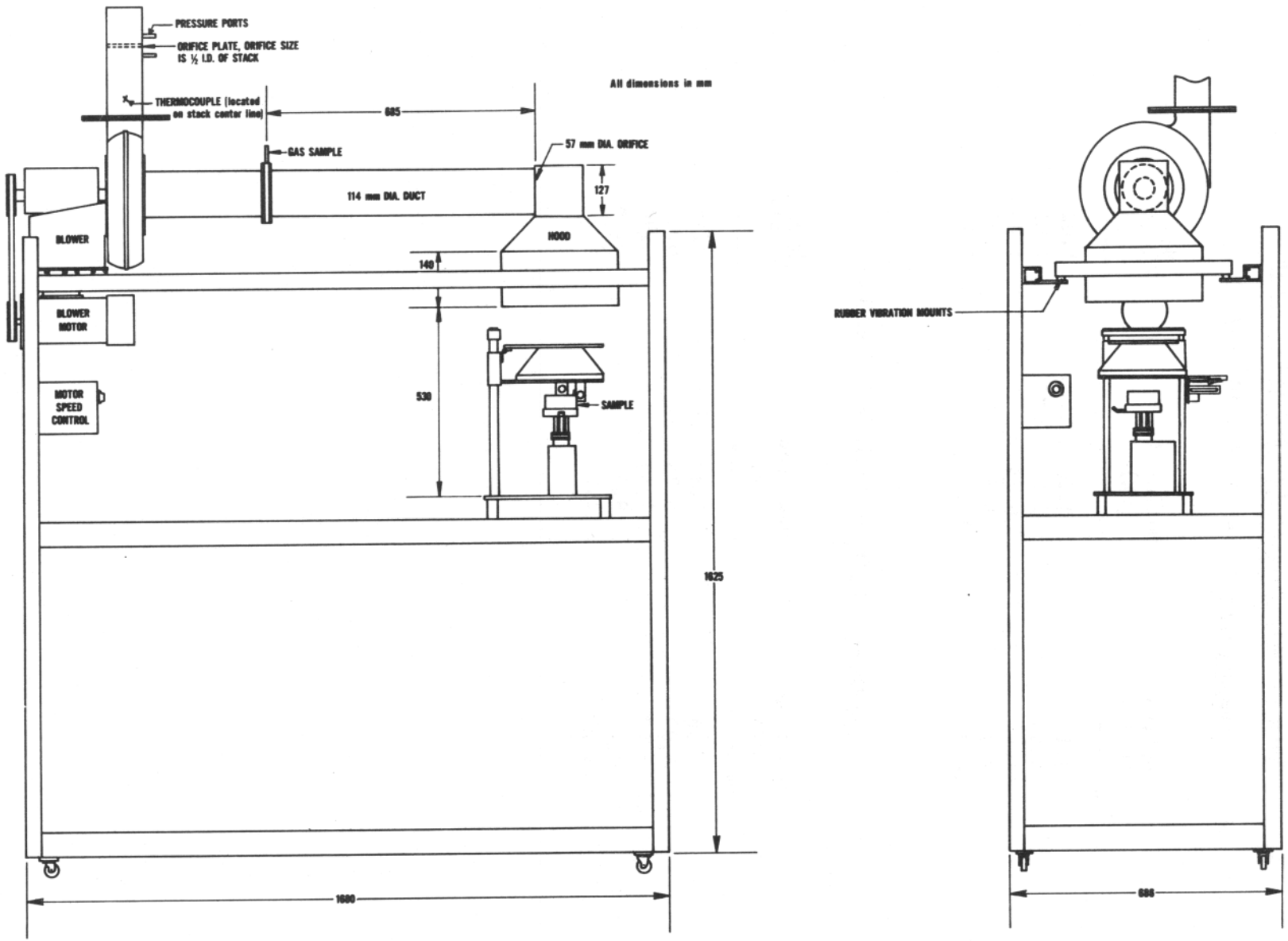

Figure 1. Over-all view of apparatus

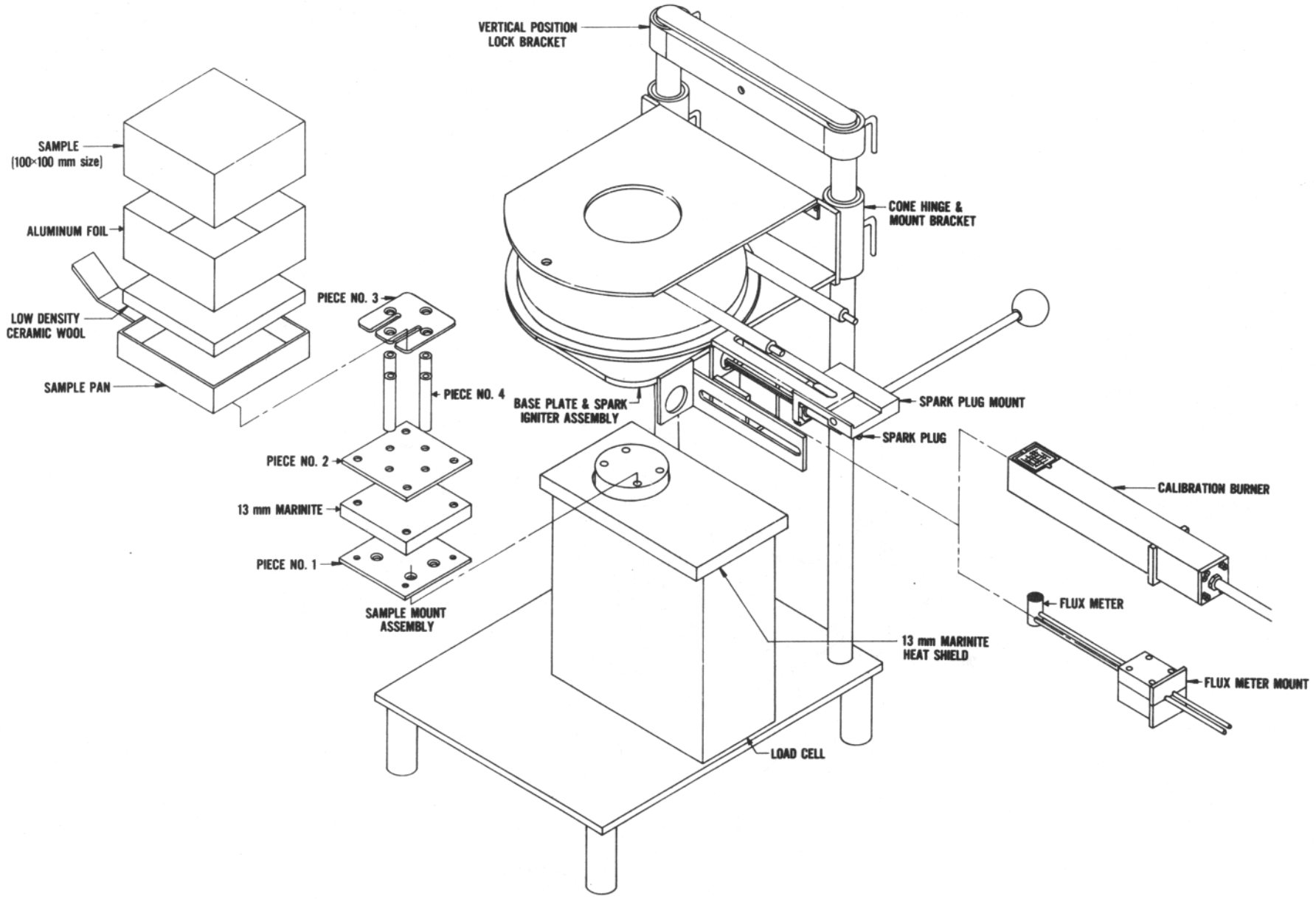

Figure 2. Exploded view, horizontal orientation

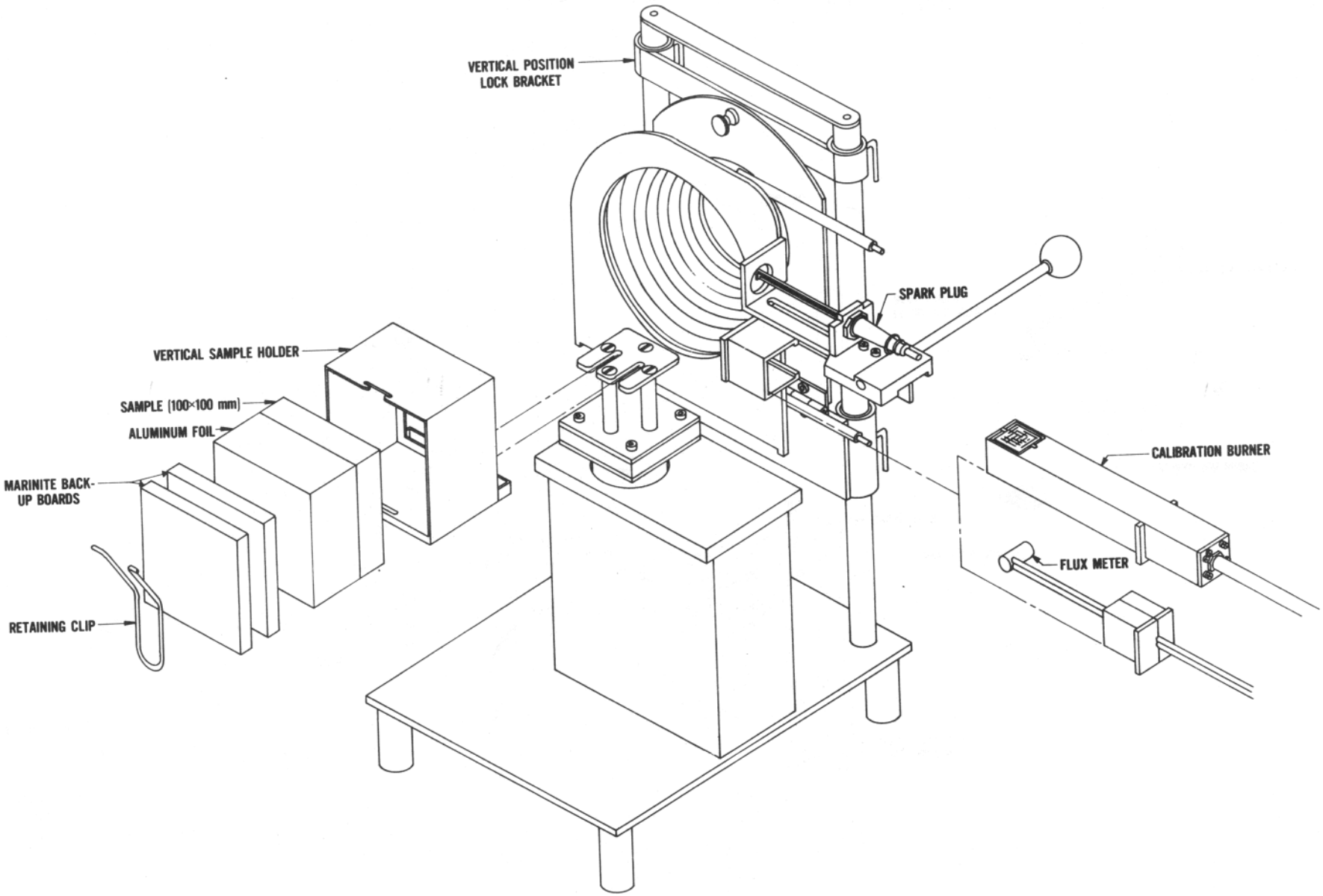

Figure 3. Exploded view, vertical orientation

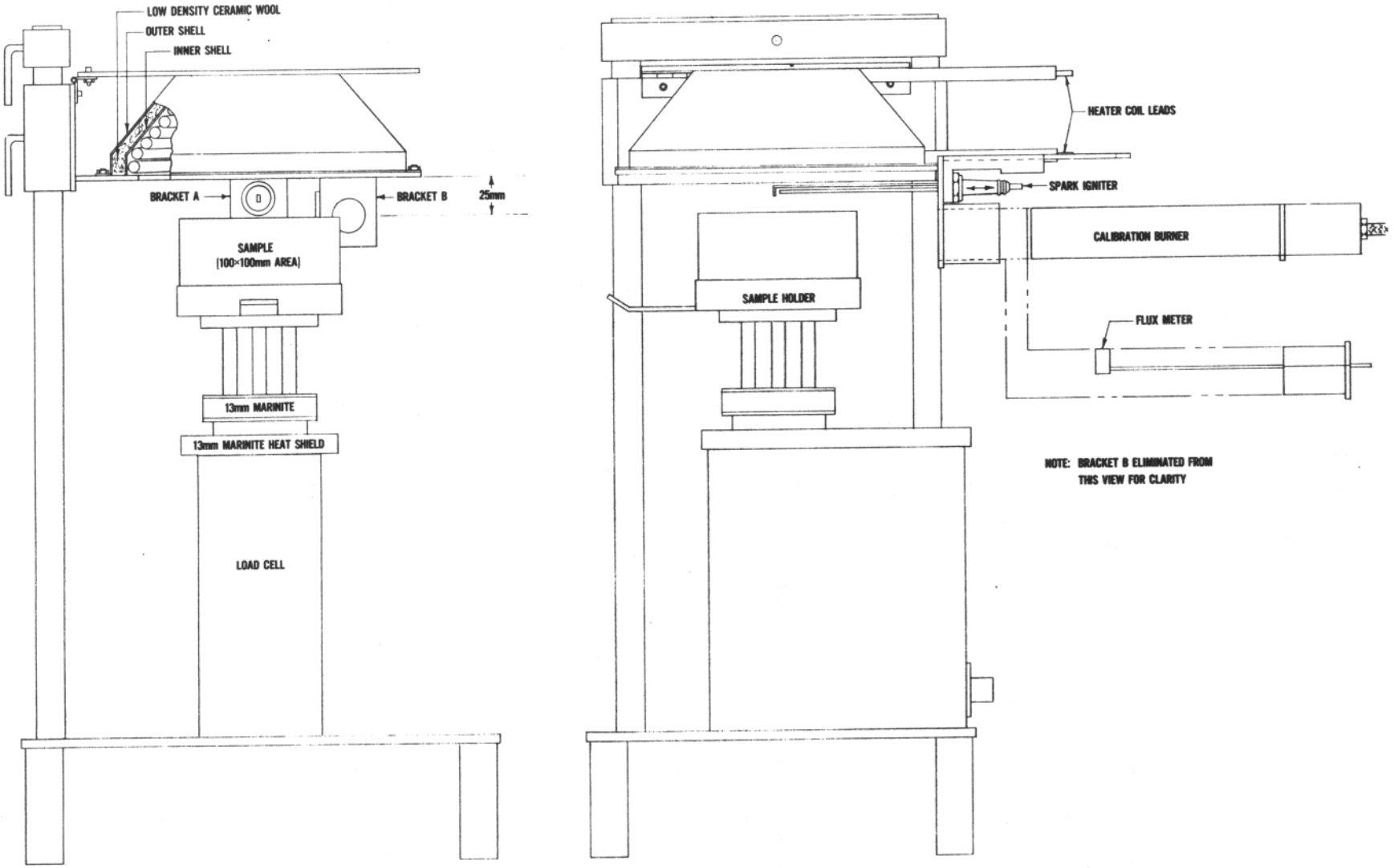

Figure 4. Elevation and side views, horizontal orientation

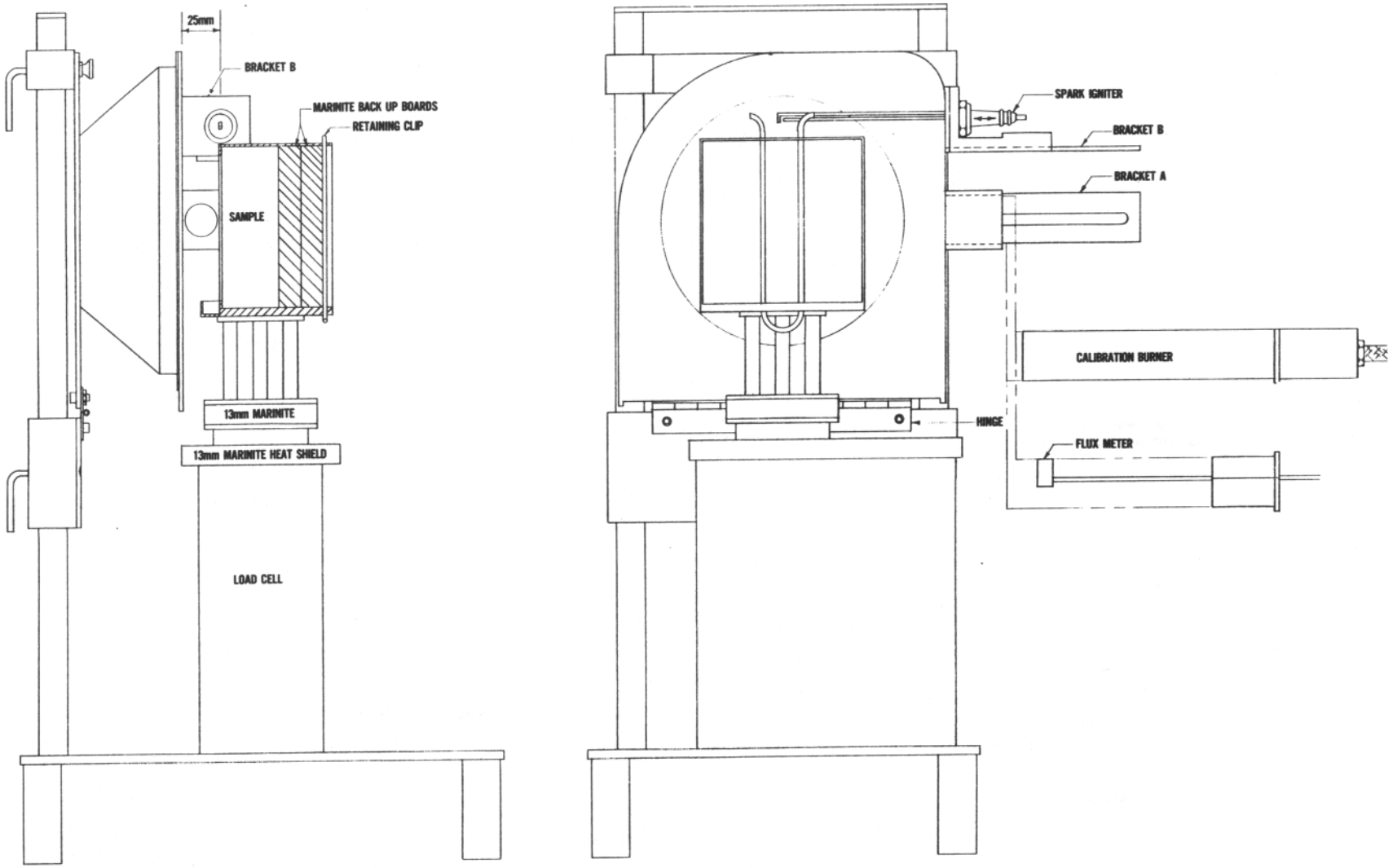

Figure 5. Elevation and side views, vertical orientation

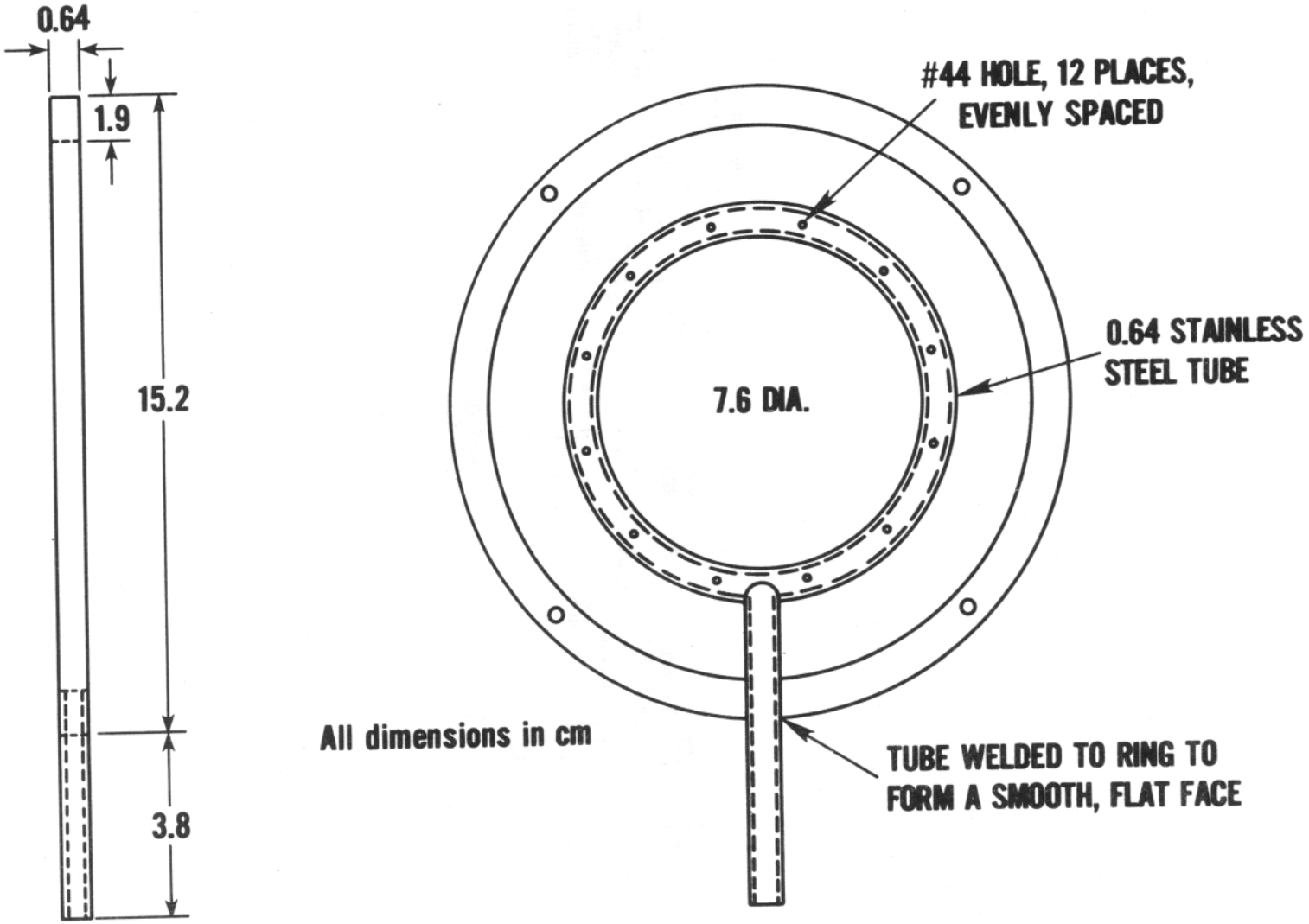

Figure 6. Gas sampling ring probe

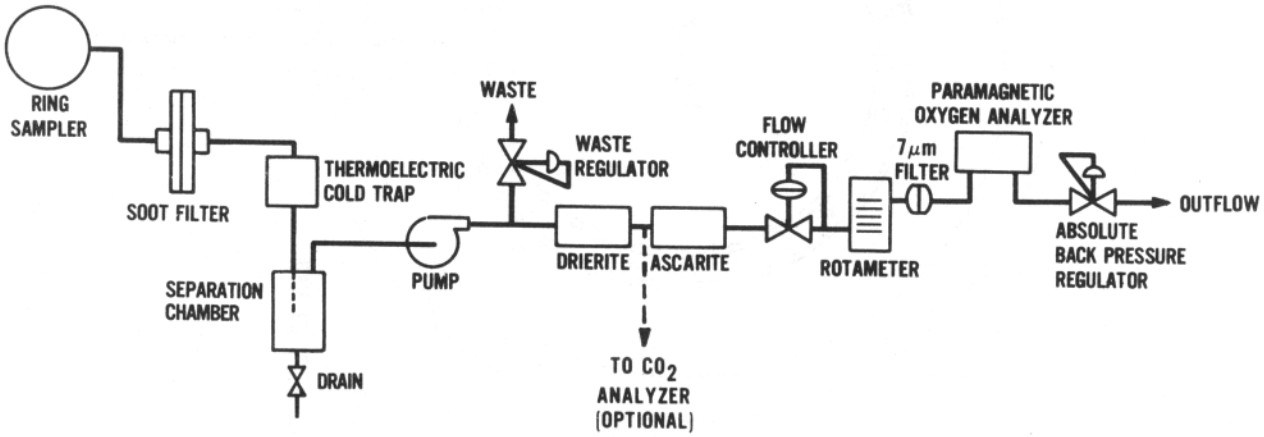

Figure 7. Gas analyzer instrumentation

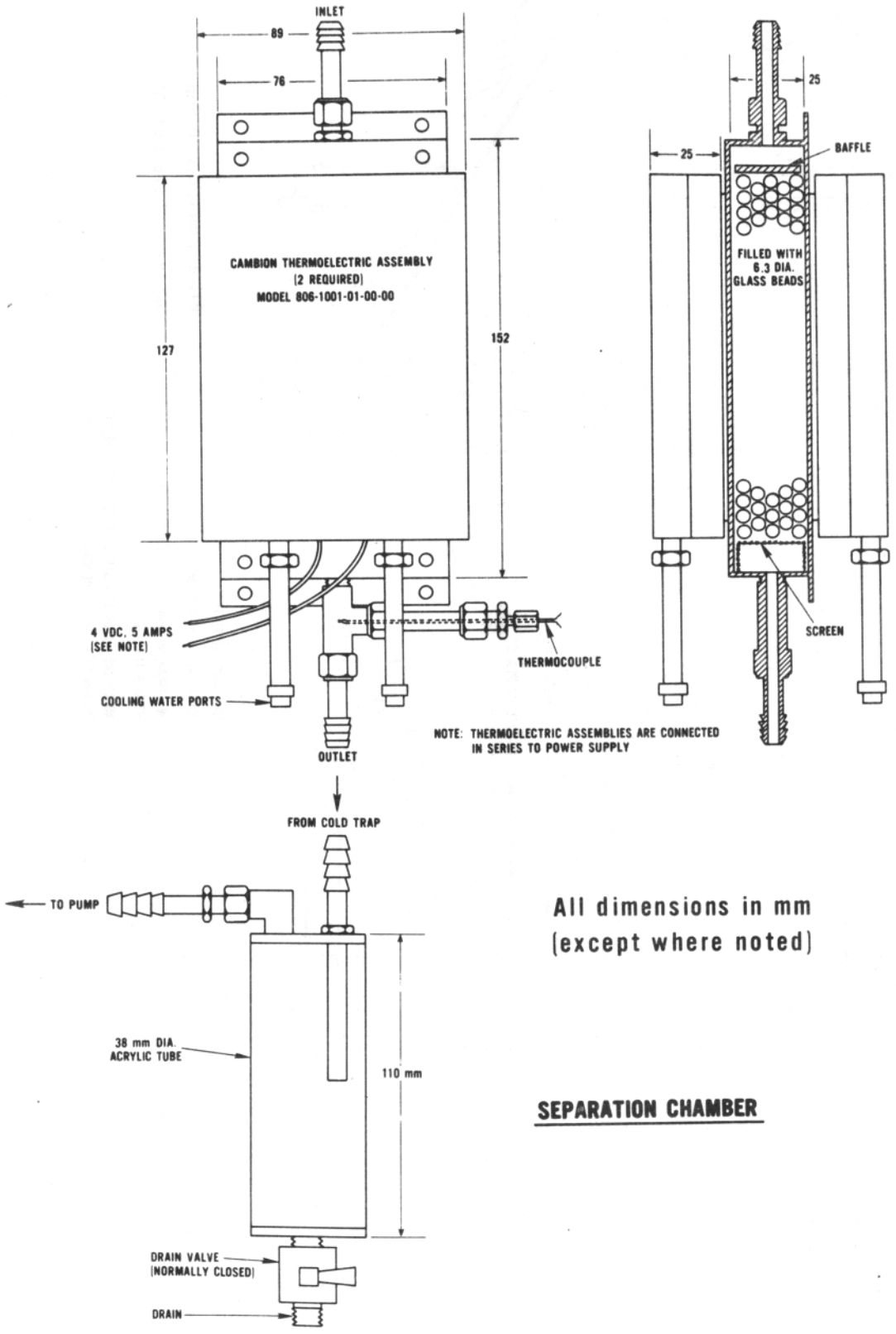

Figure 8. Thermoelectric cold trap

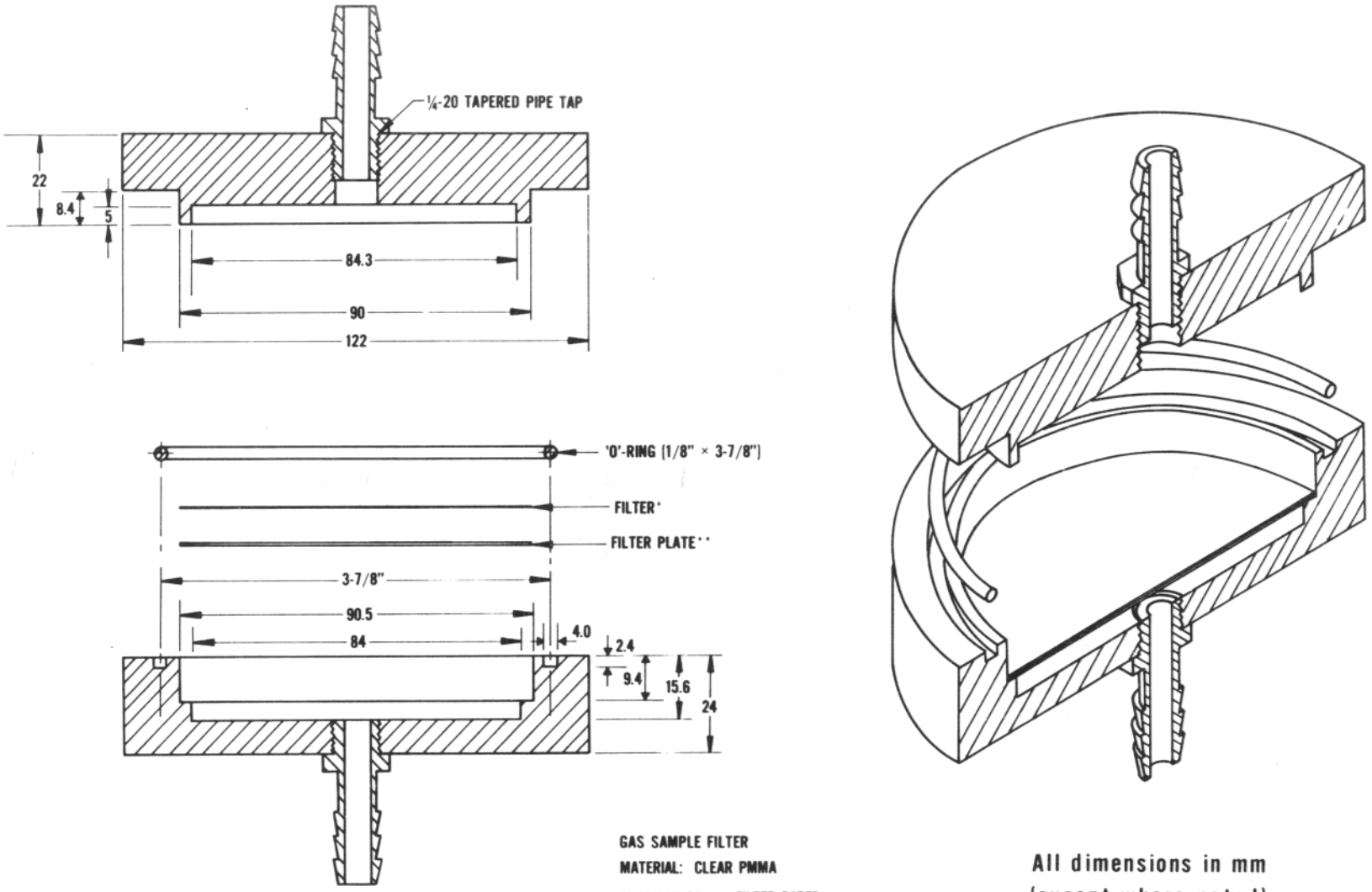

Figure 9. Soot filter

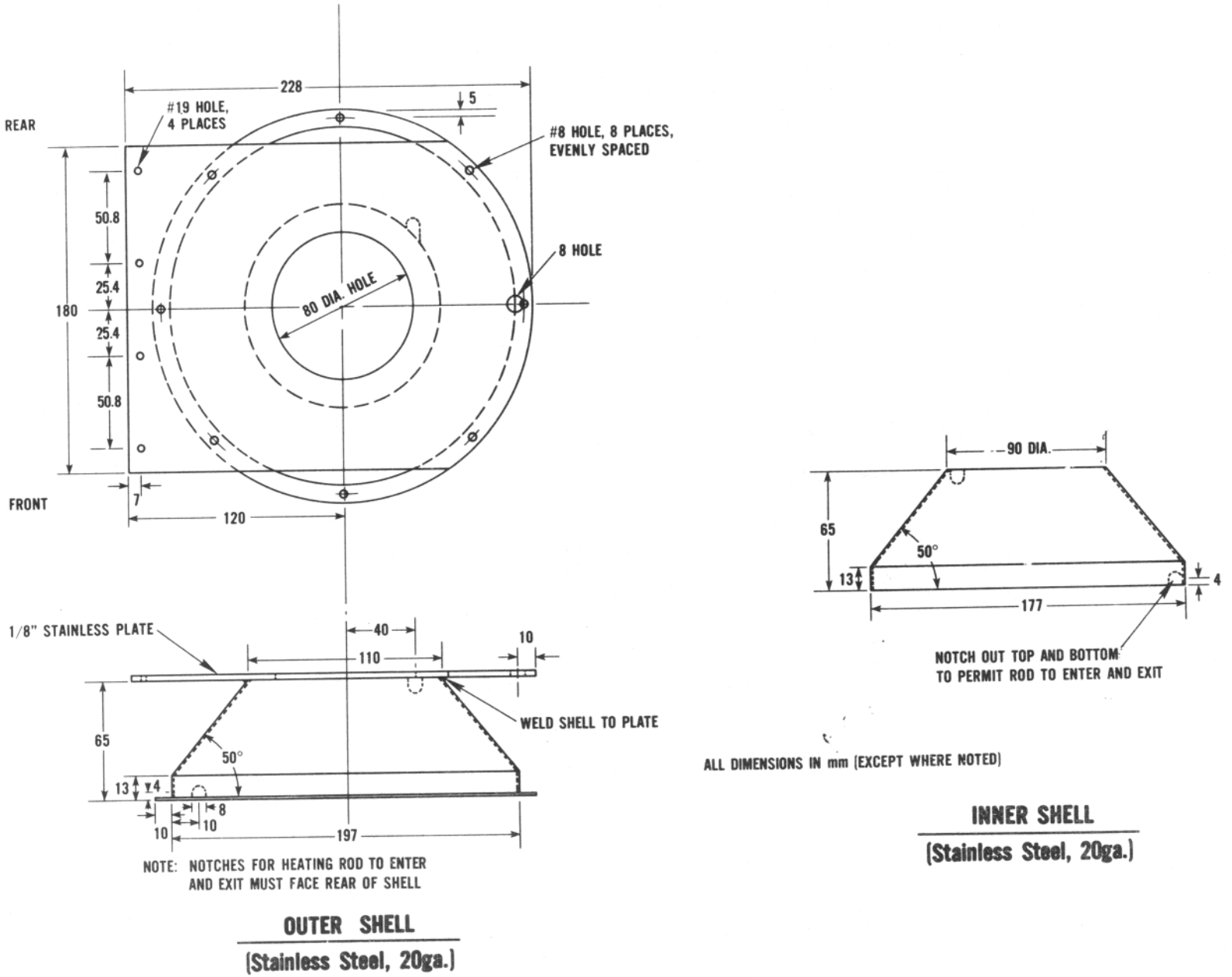

Figure 10. Inner and outer shells for cone heater

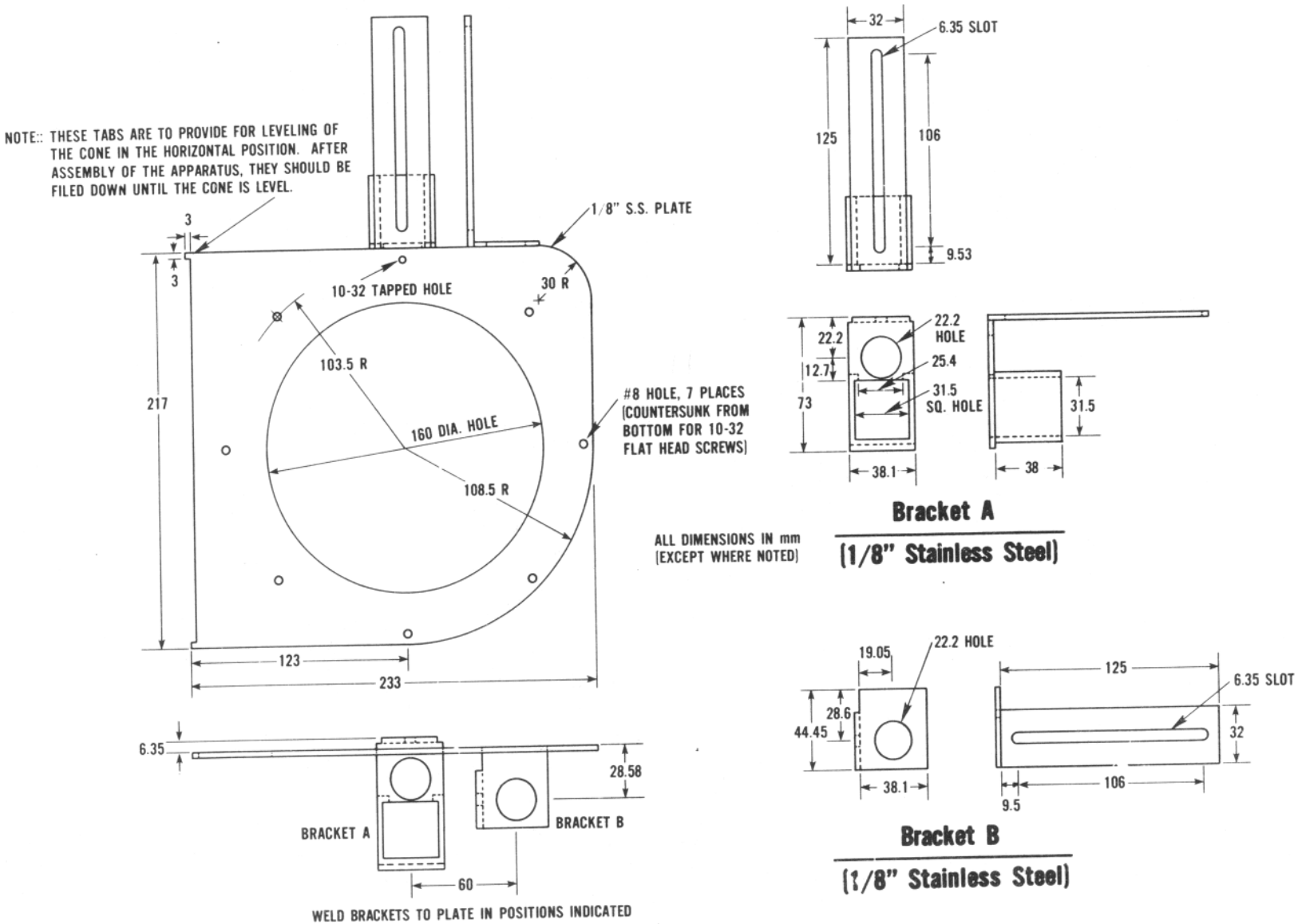

Figure 11. Base plate and brackets for cone heater

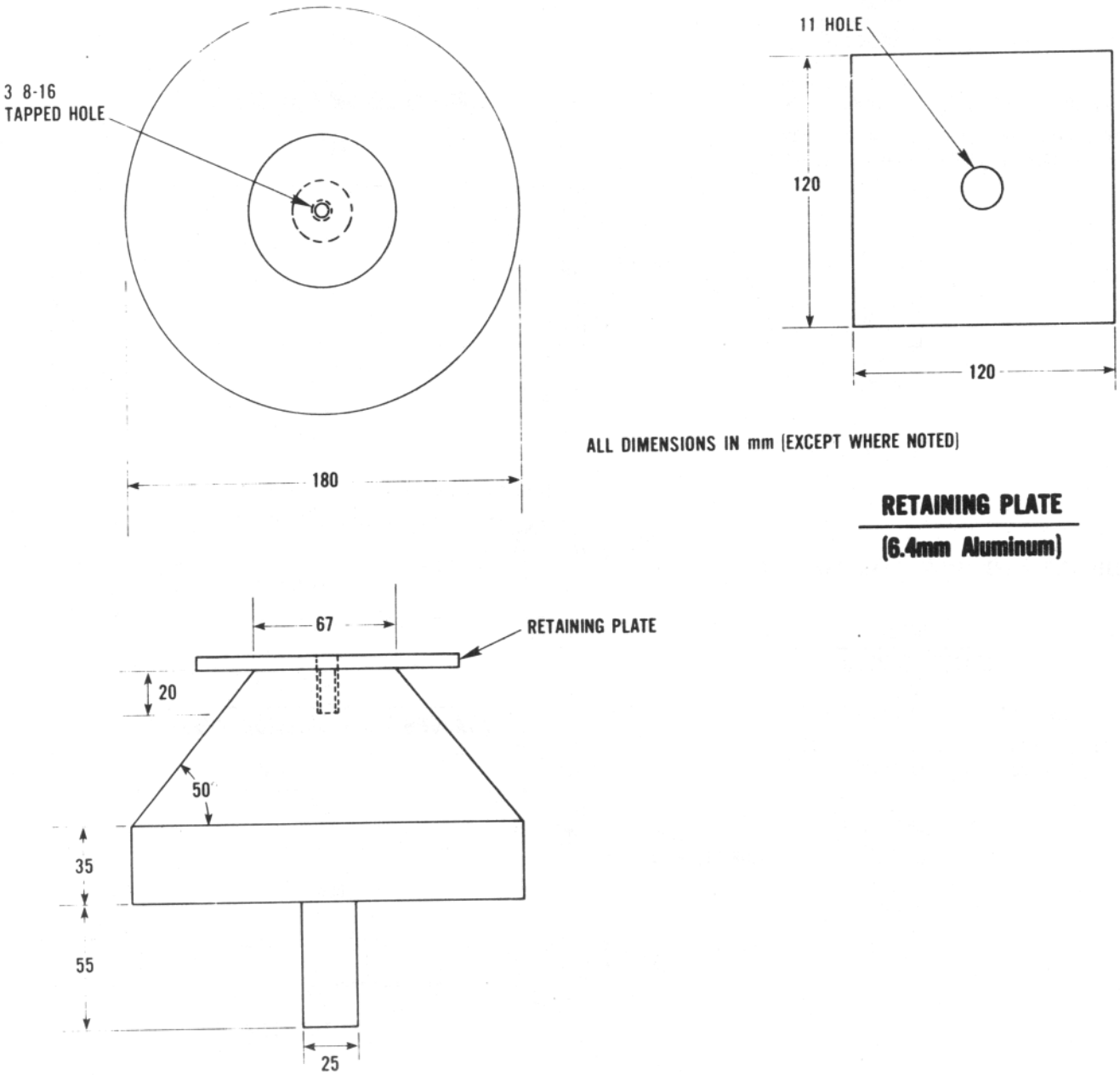

Figure 12. Mandrel for winding cone heater

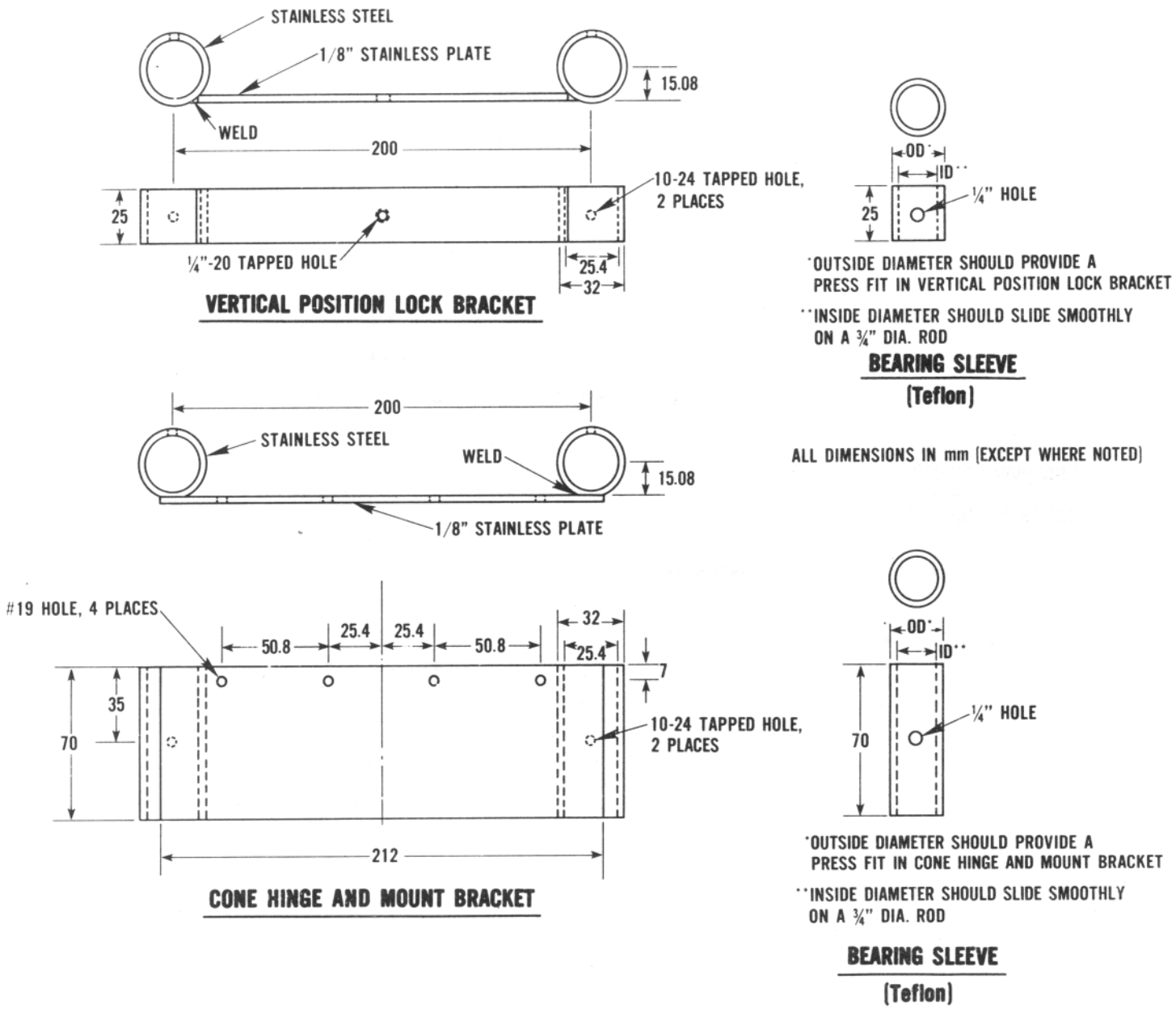

Figure 13. Sliding cone support brackets

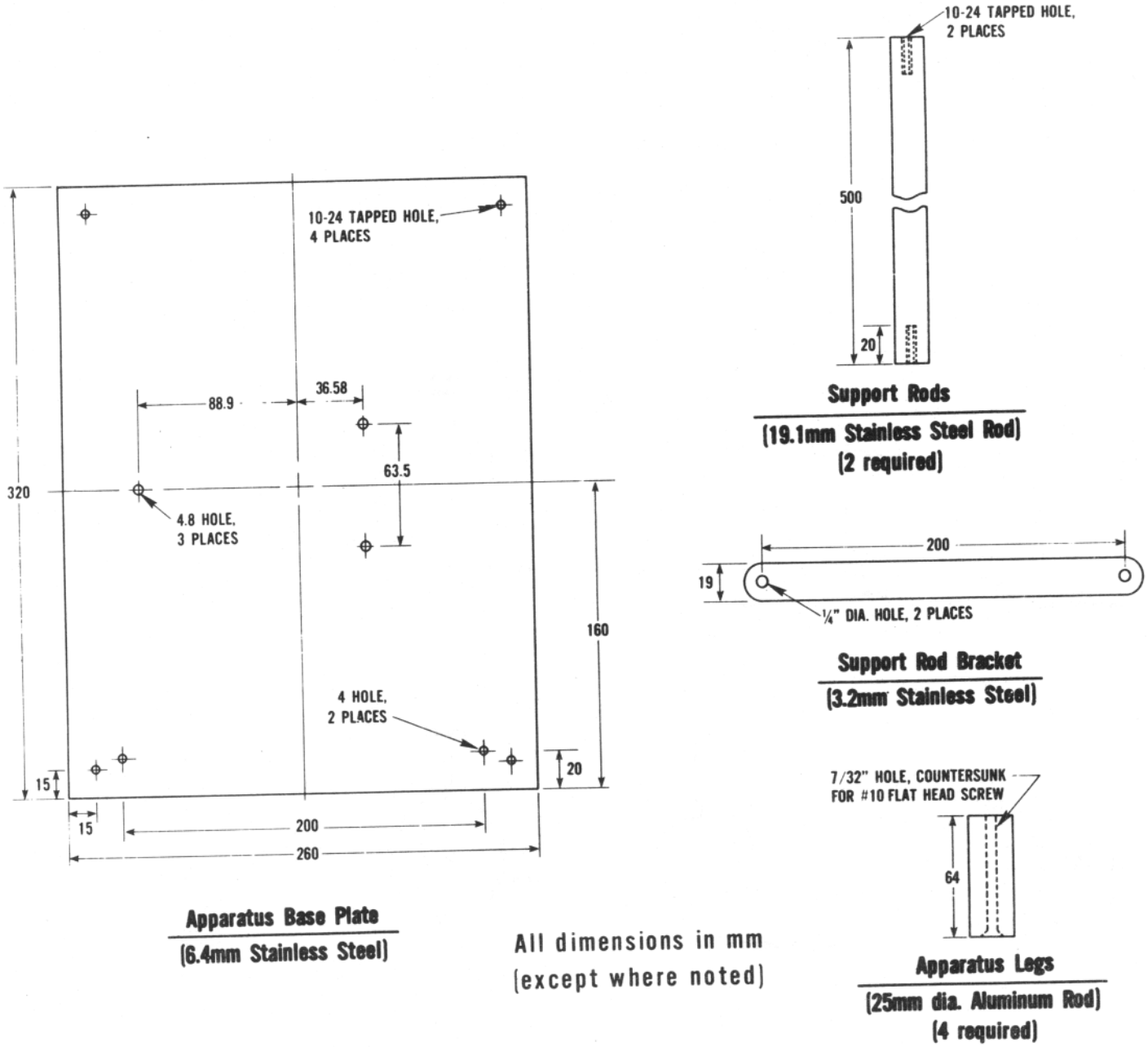

Figure 14. Base plate and support pieces

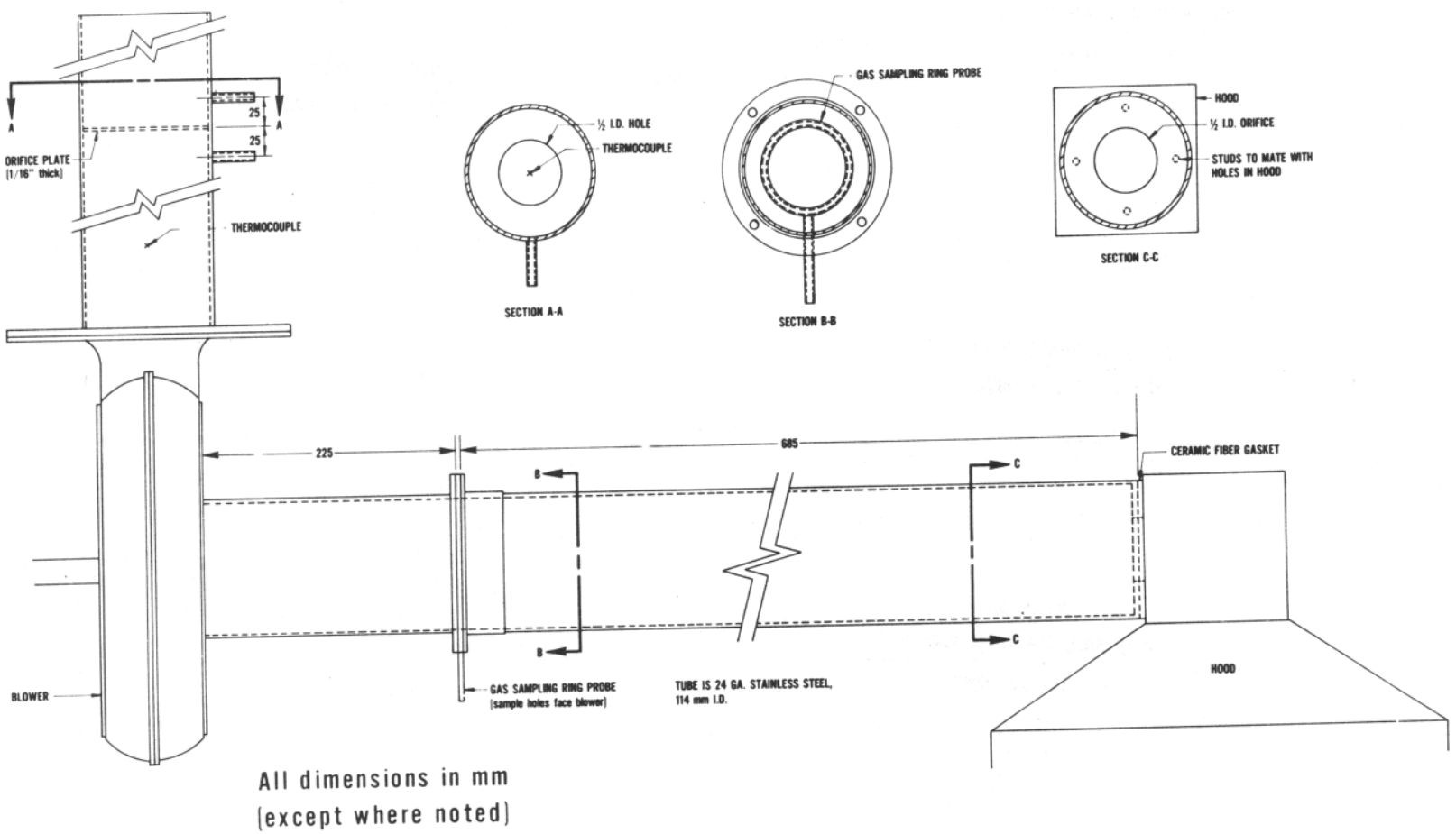

Figure 15. Exhaust system

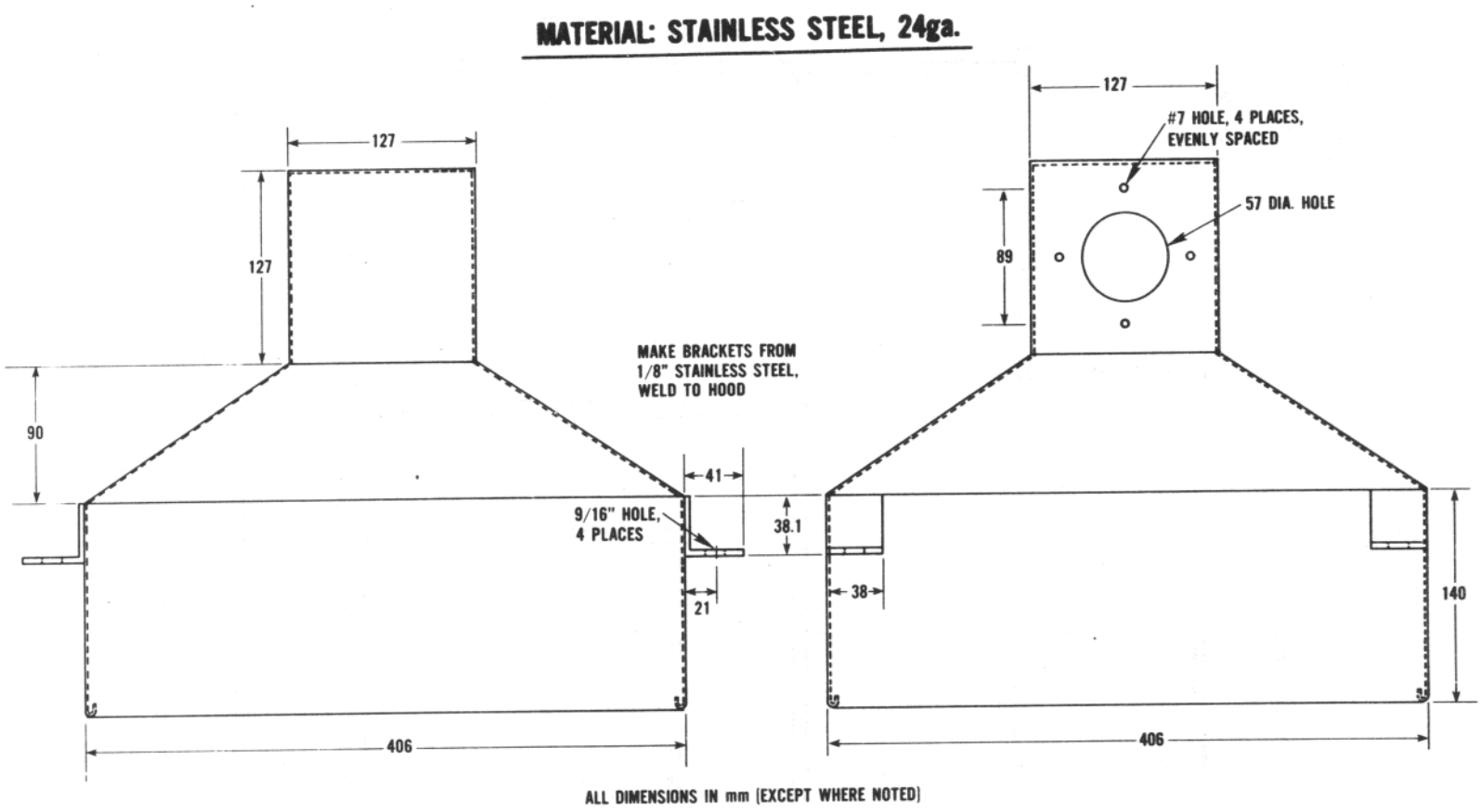

Figure 16. Exhaust duct

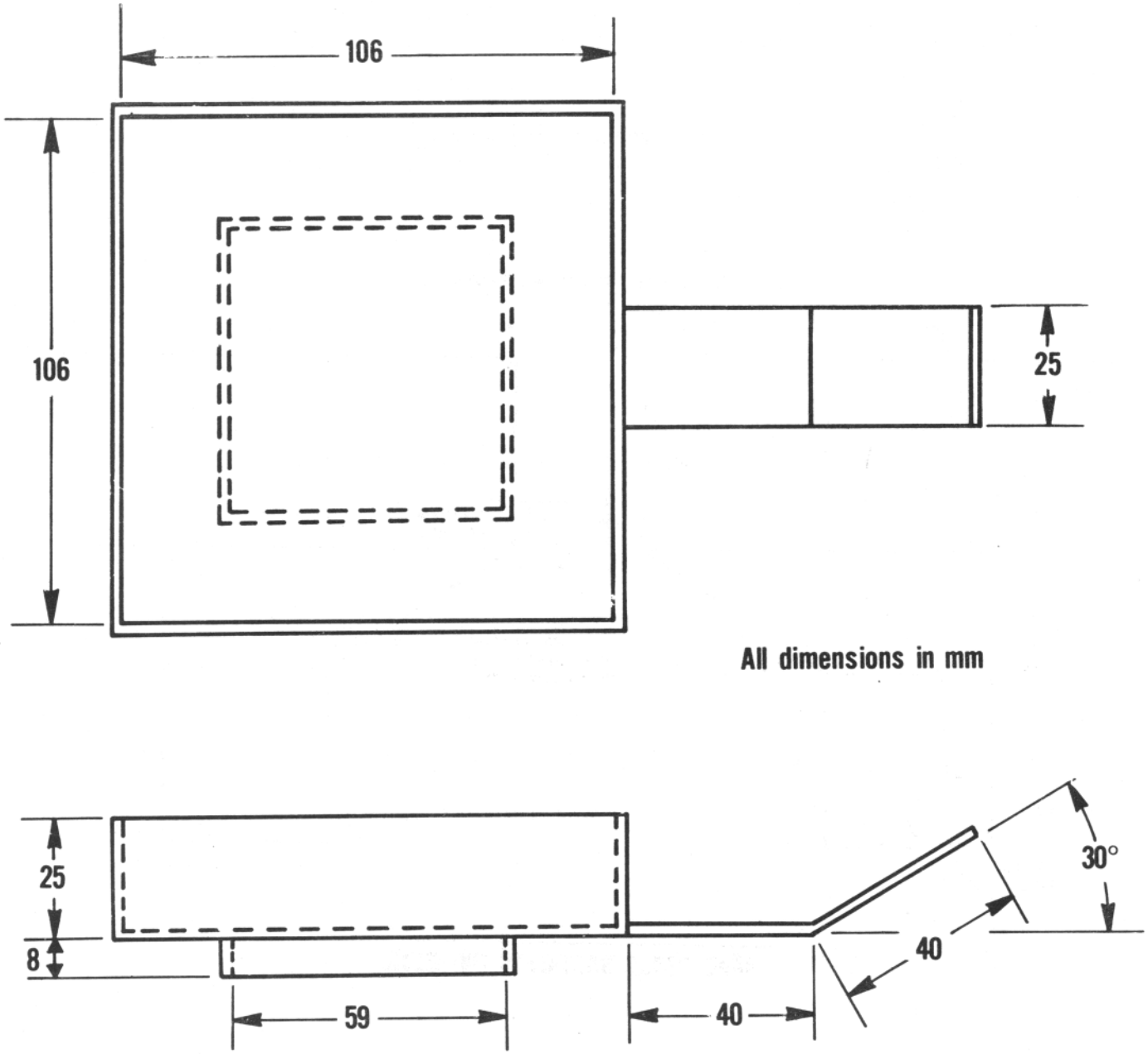

Figure 17. Horizontal specimen holder

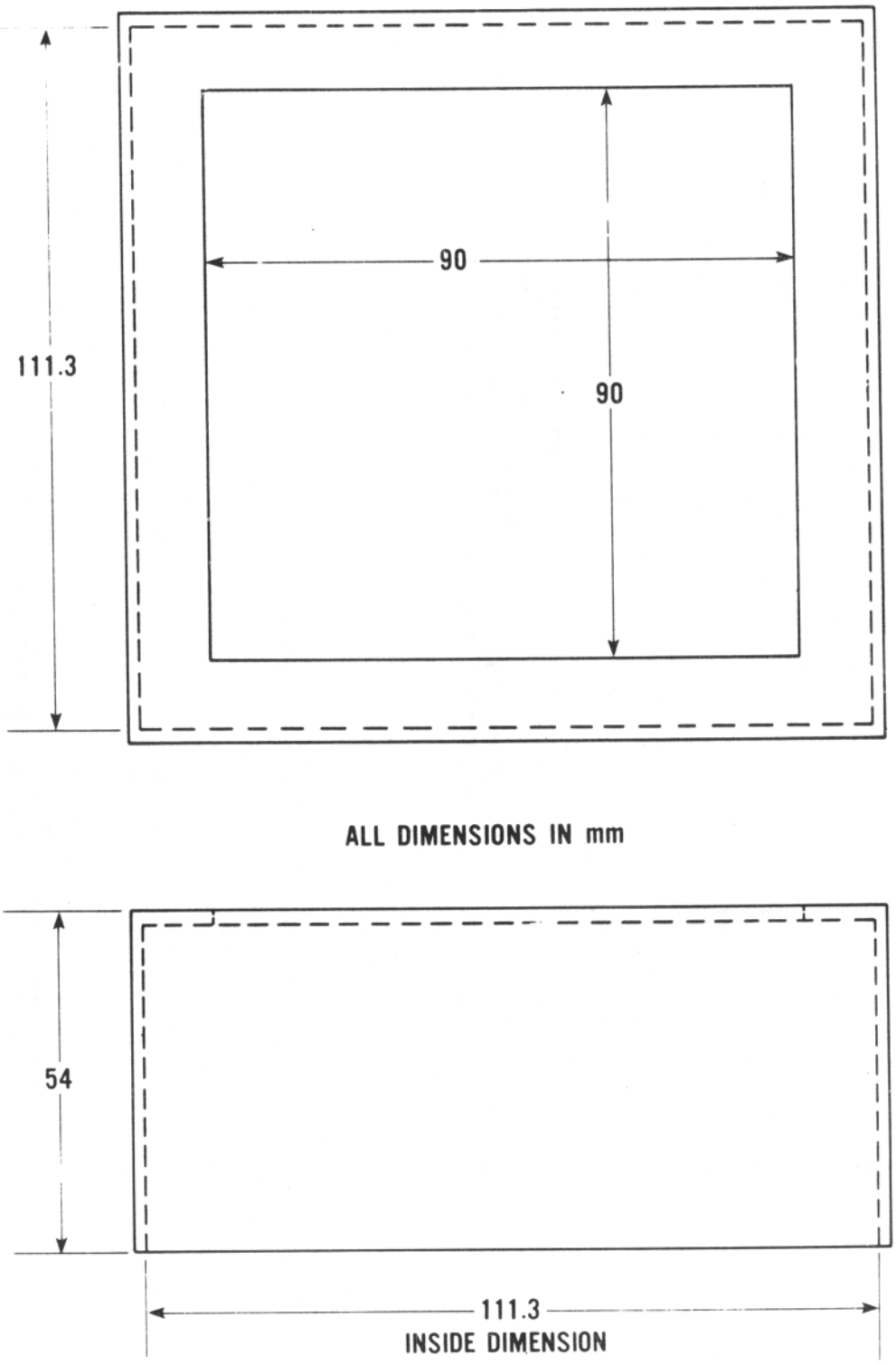

Figure 18. Retainer frame for horizontal ignitability testing

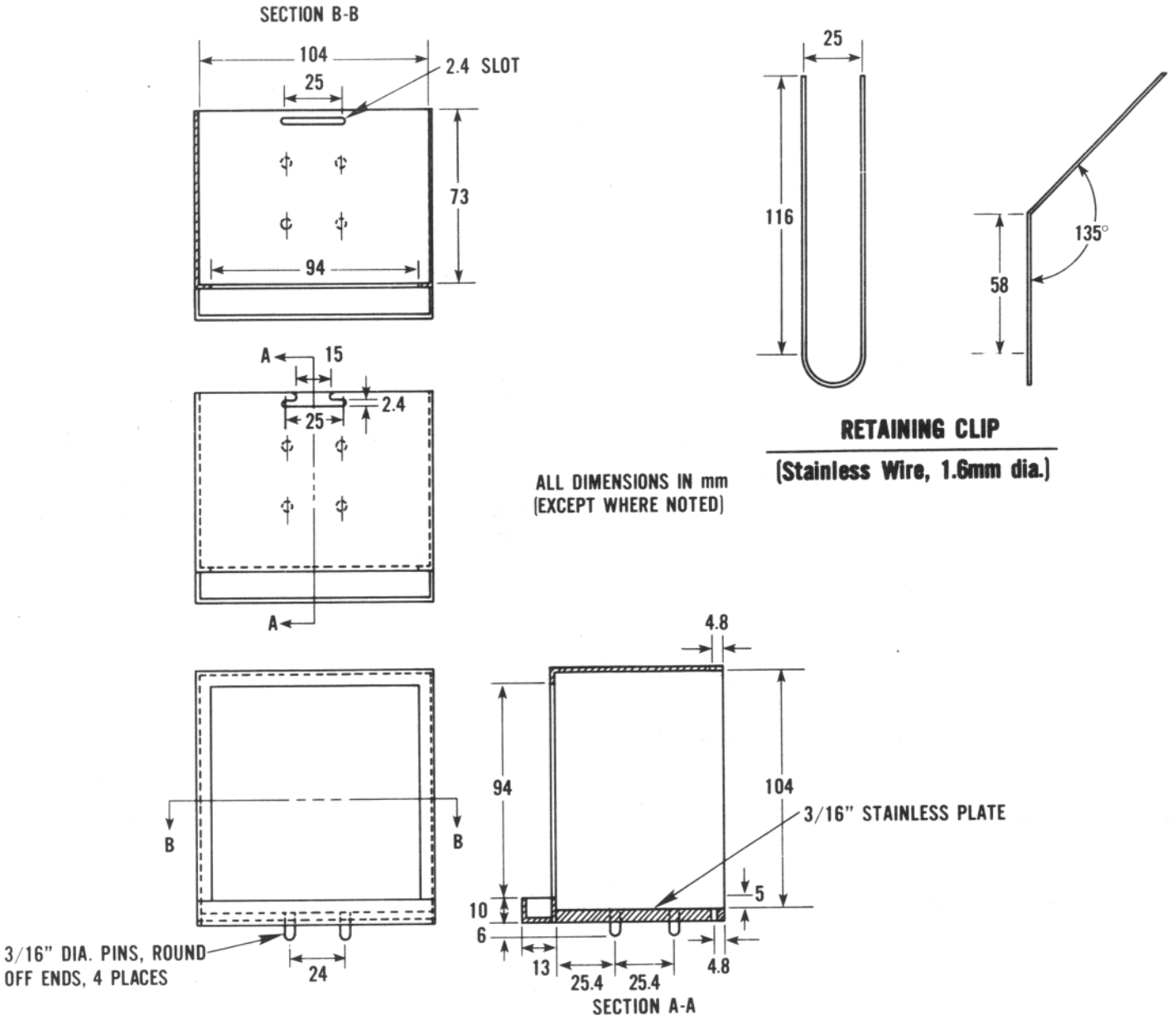

Figure 19. Vertical specimen holder

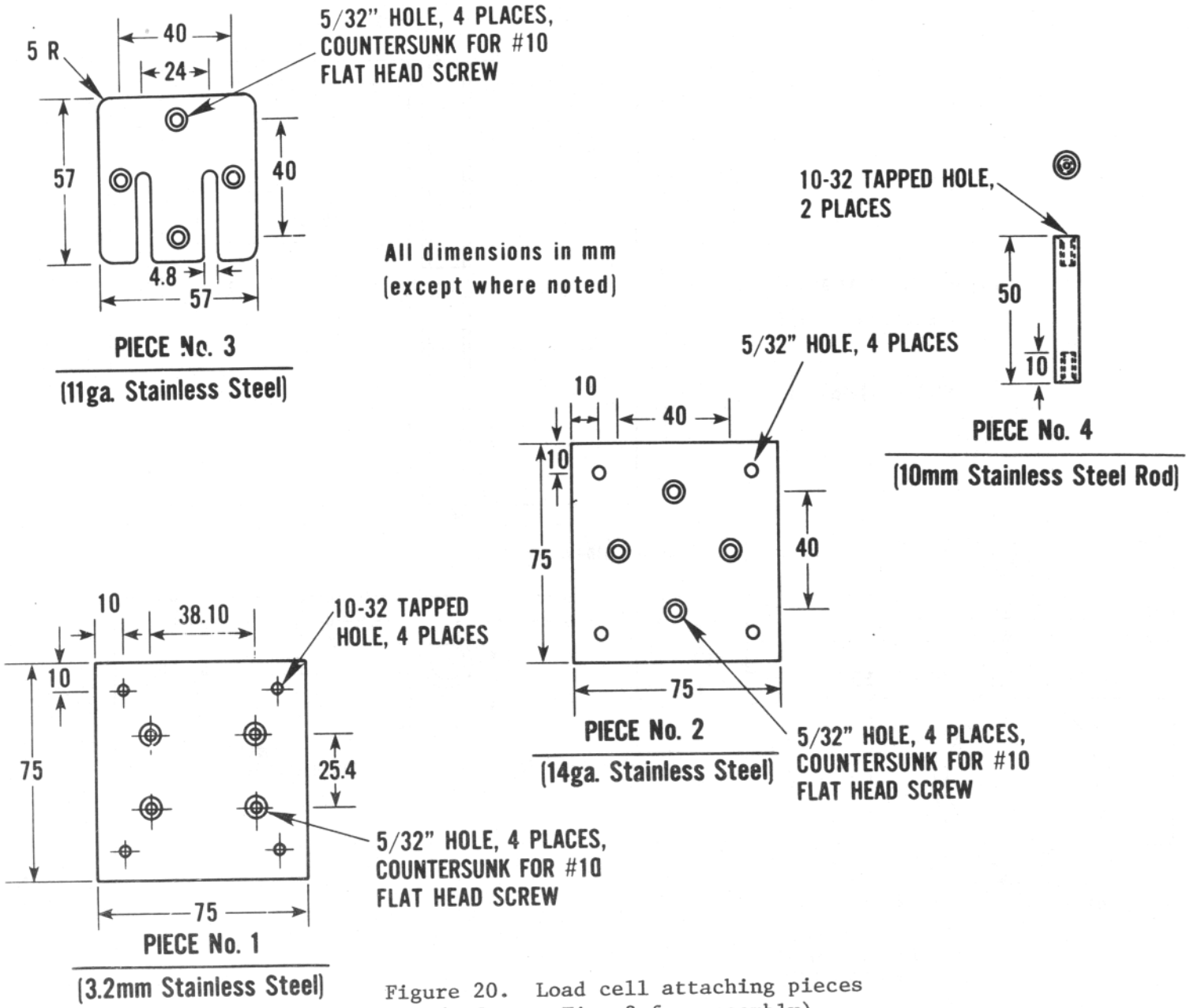

Figure 20. Load cell attaching pieces
(refer to Fig. 2 for assembly)

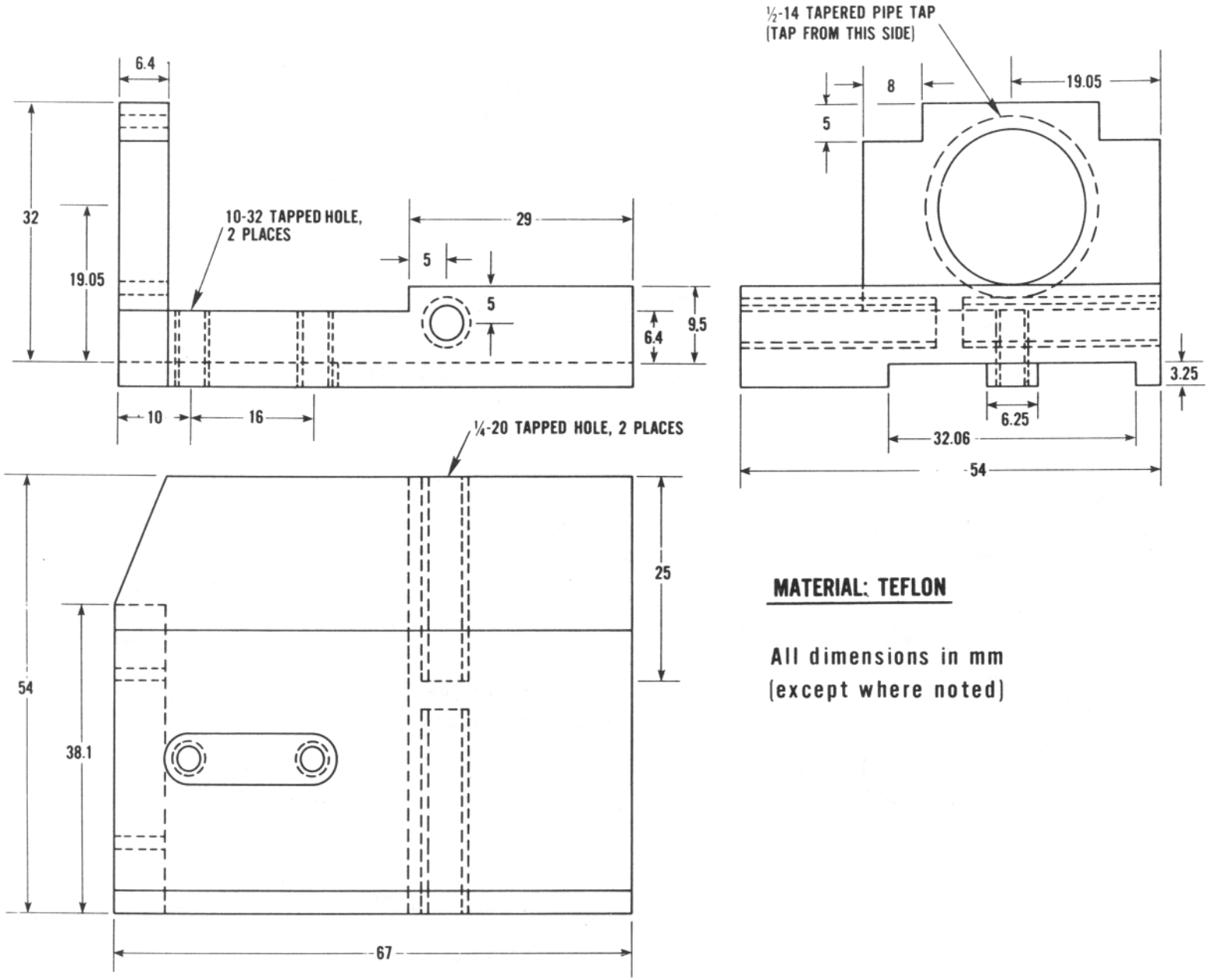

Figure 21. Spark plug carrier

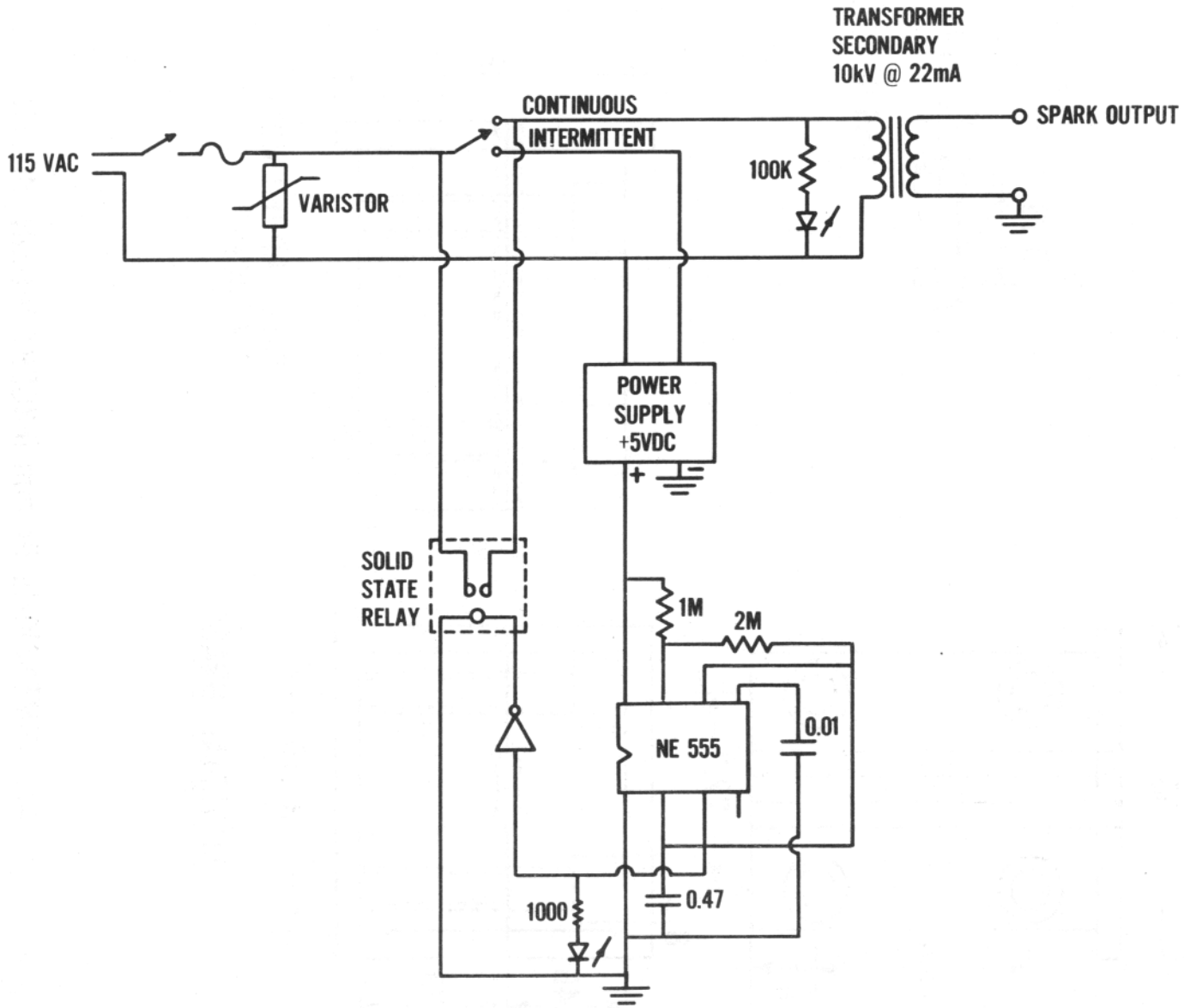

Figure 22. Power supply for spark plug

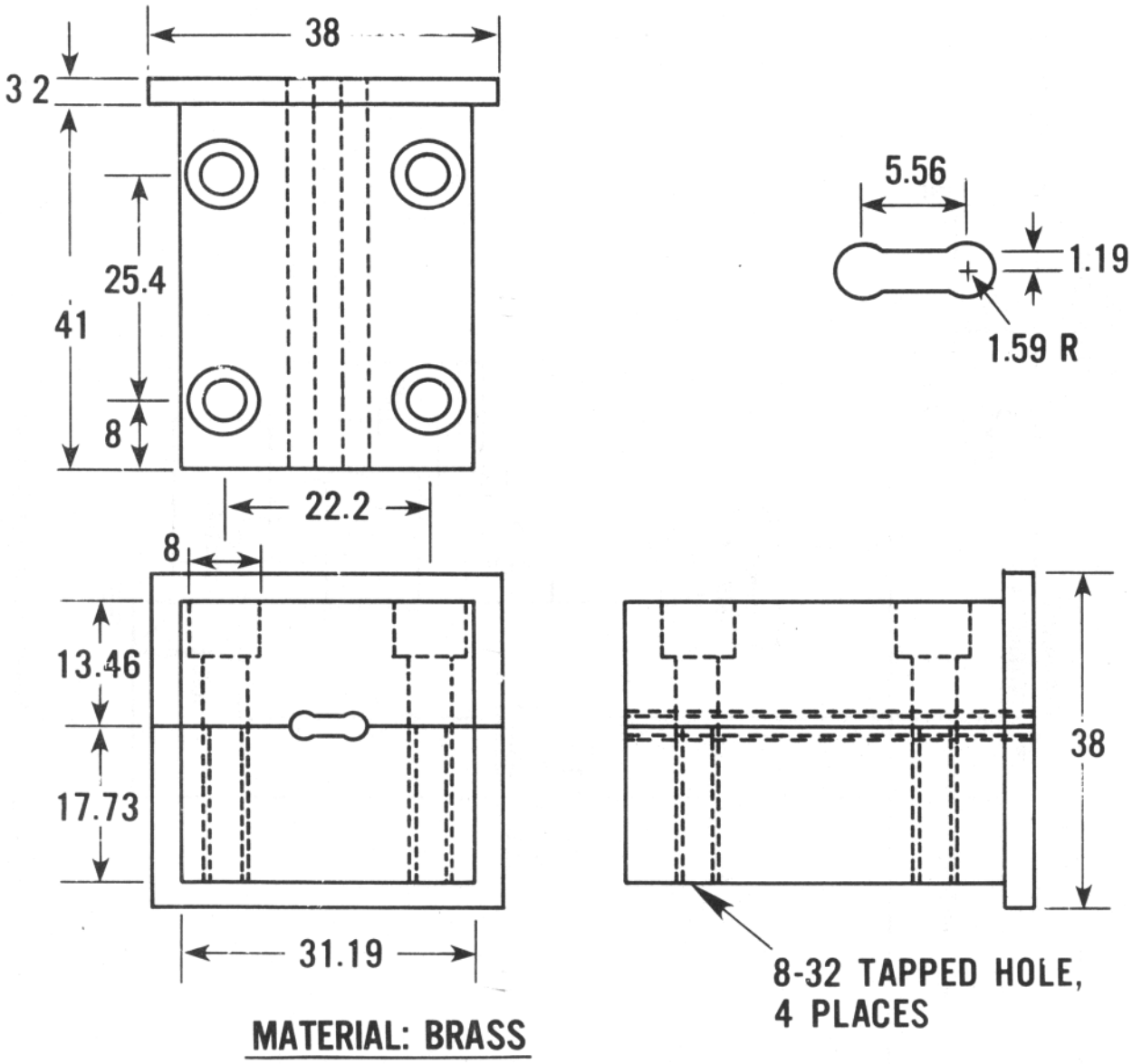

ALL DIMENSIONS IN mm (EXCEPT WHERE NOTED)

Figure 23. Holder for Gardon gage

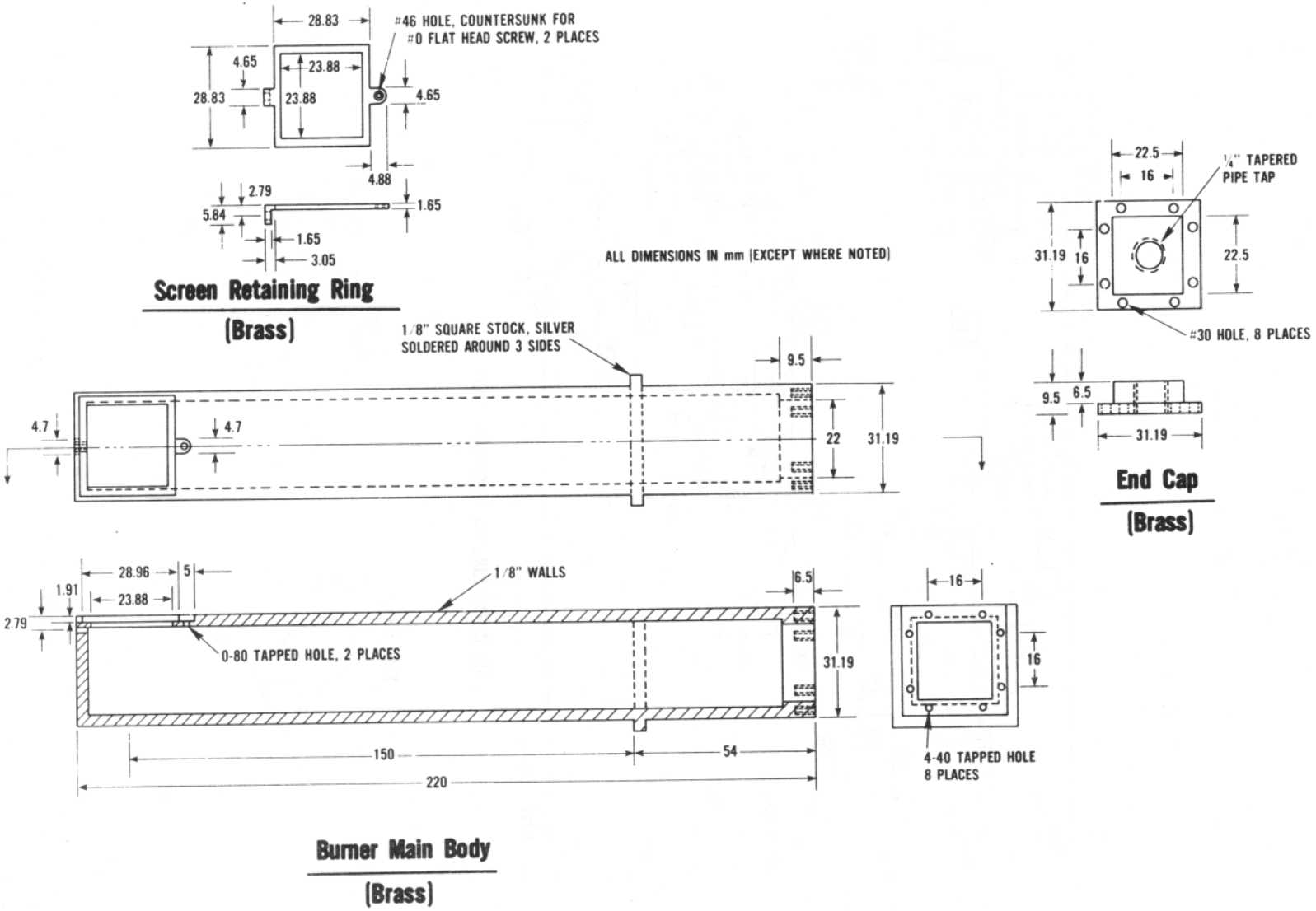

Figure 24. Calibration Burner

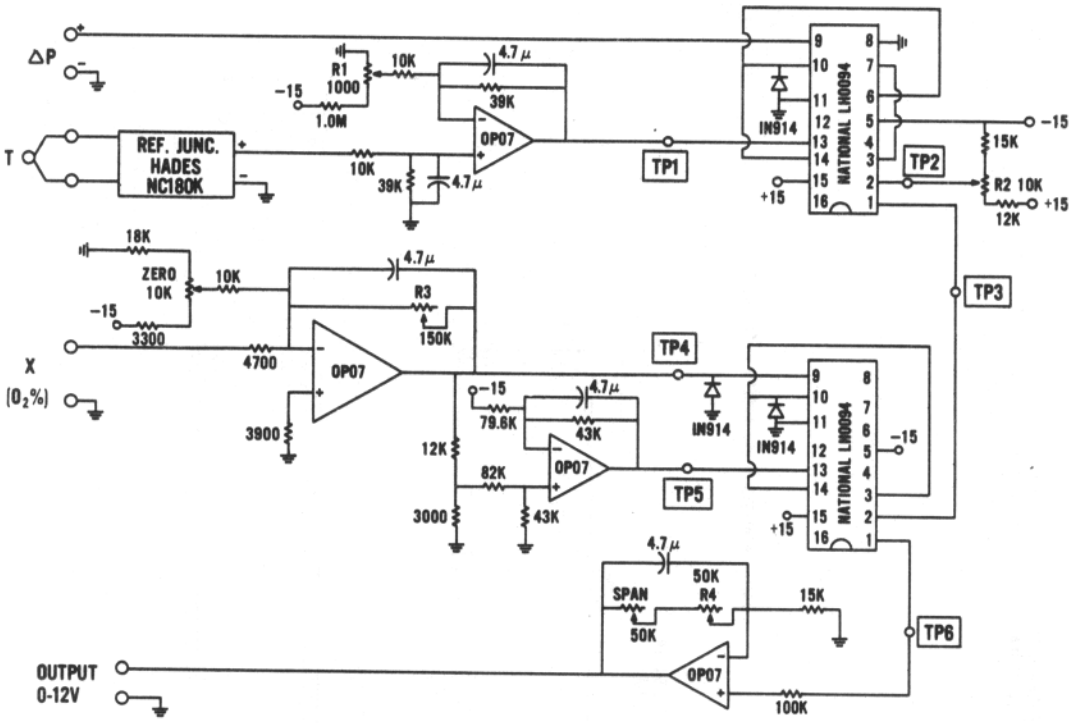

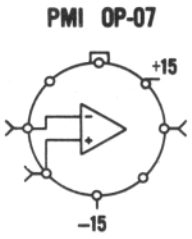

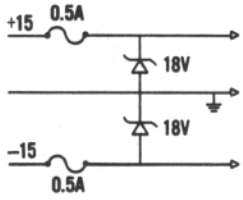

Figure 25. Analog signal module

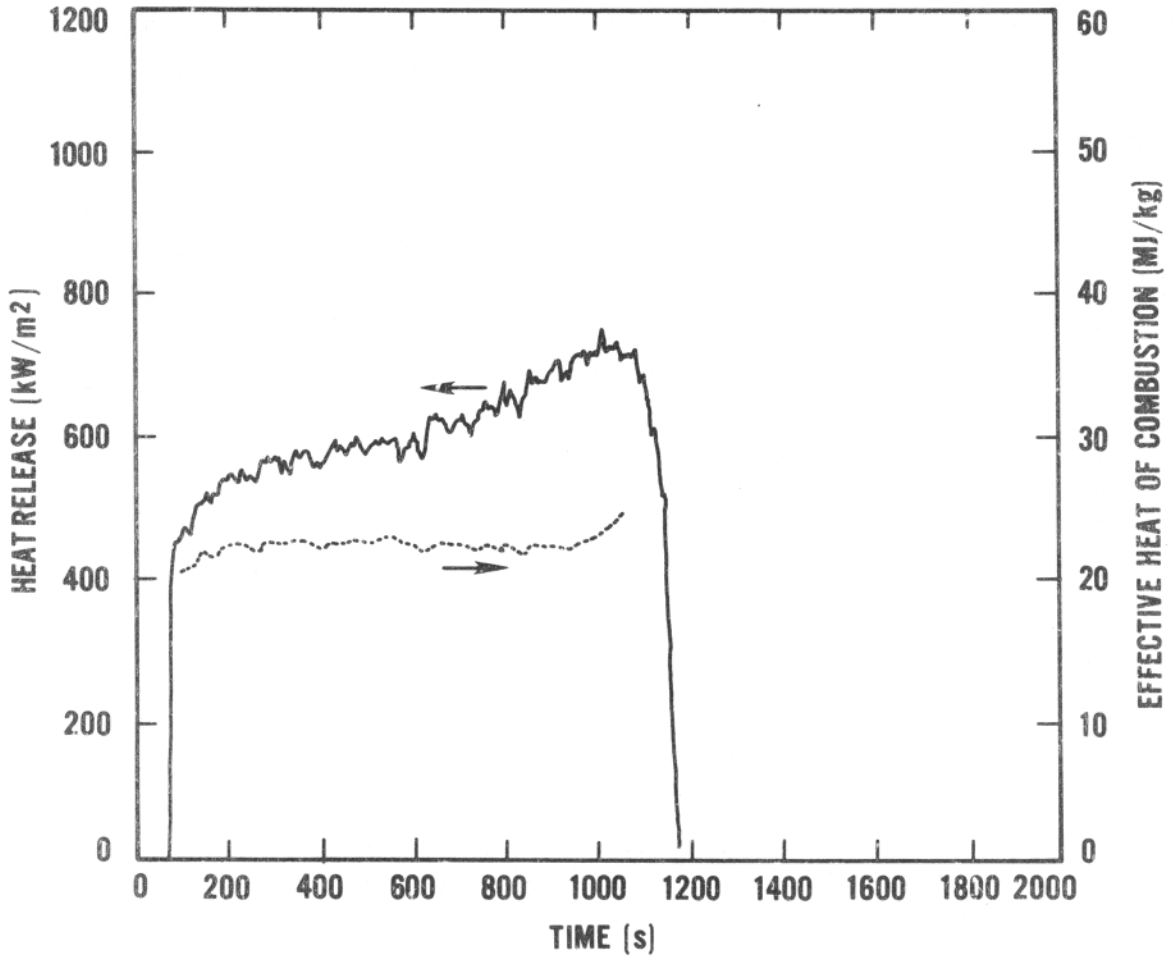

Figure 26. PMMA (horizontal) rate of heat release and heat of comubstion at 50 kW/m^2 irradiance

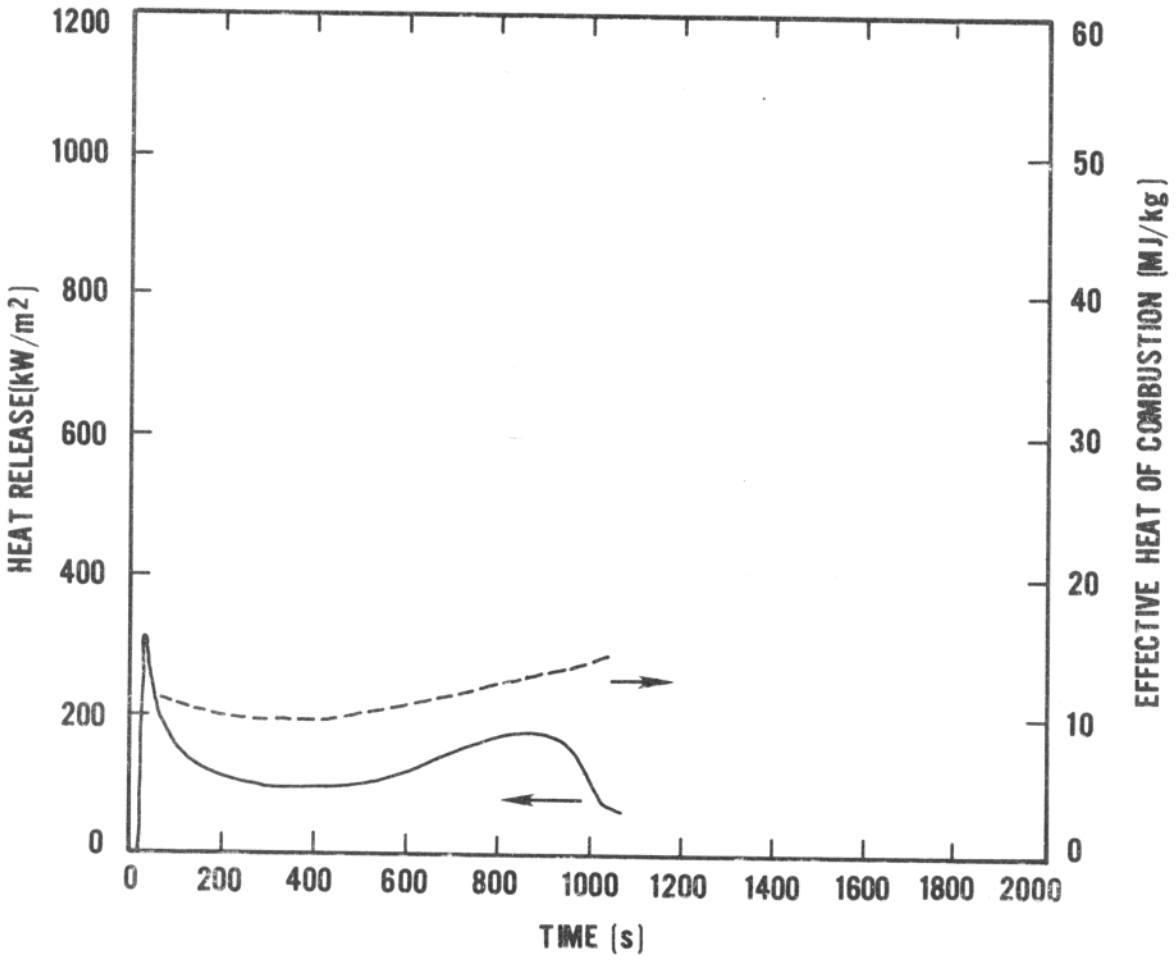

Figure 27. Red oak (horizontal) rate of heat release and heat of combustion at 50 kW/m^2 irradiance

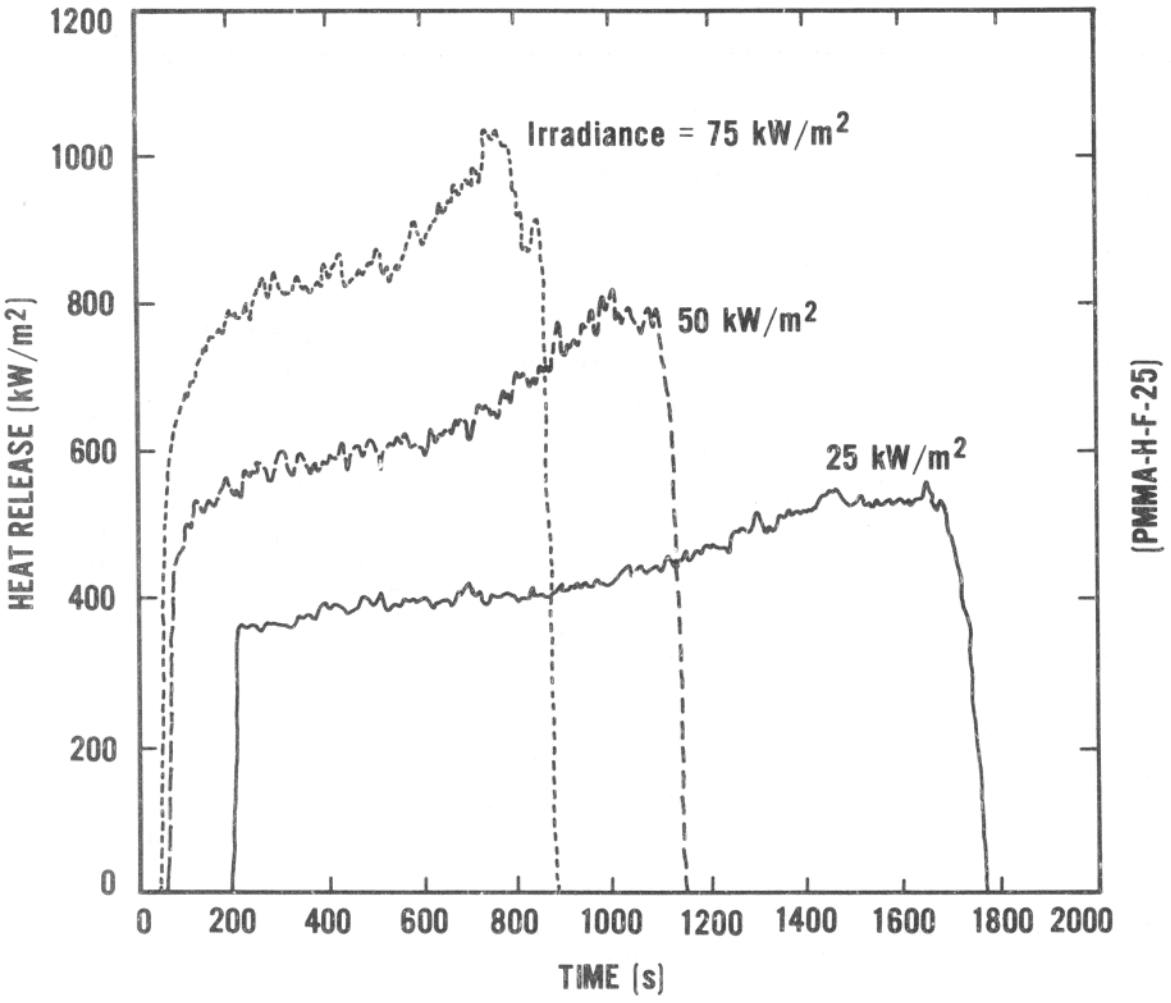

Figure 28. PMMA (horizontal) rate of heat release at several irradiances

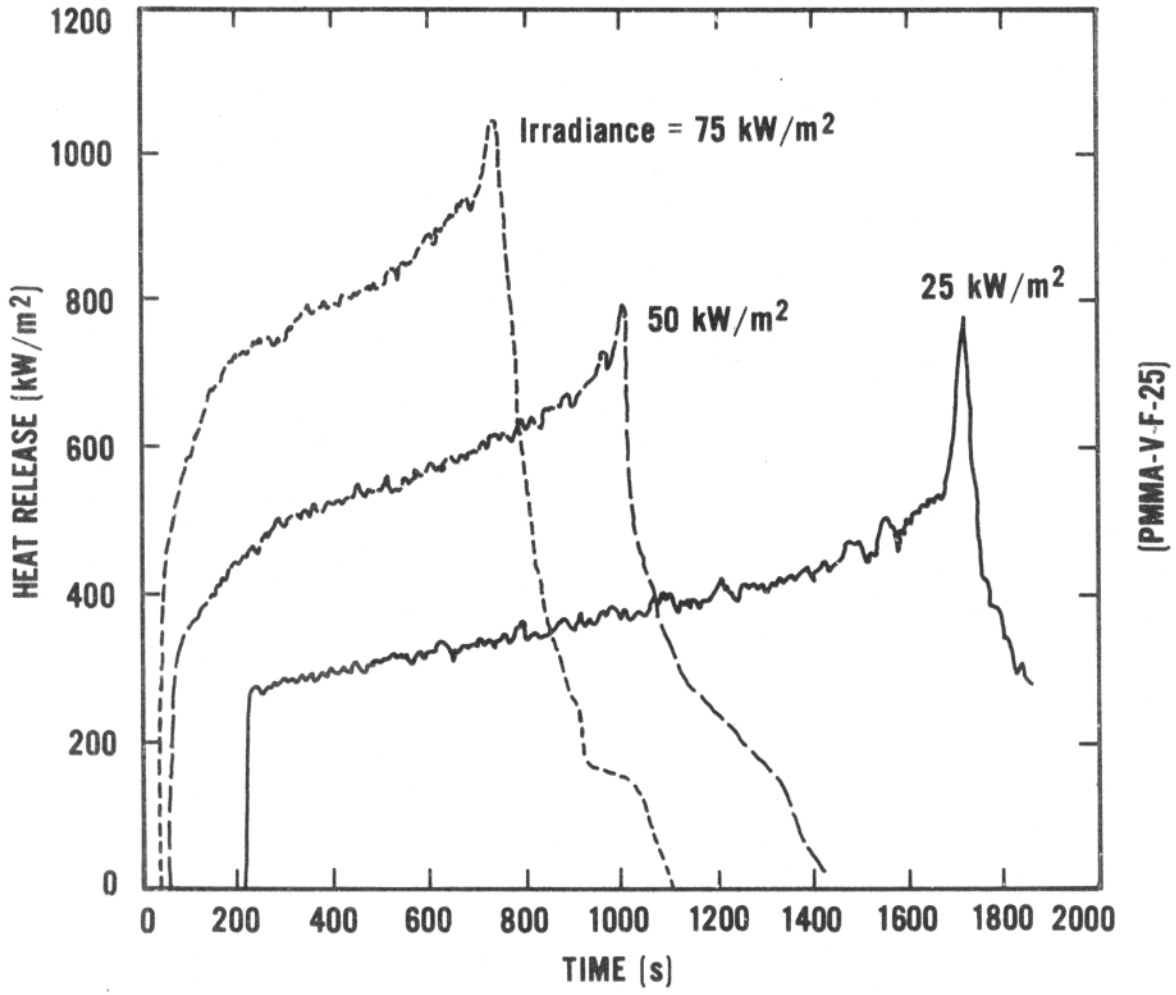

Figure 29. PMMA (vertical) rate of heat release at several irradiances

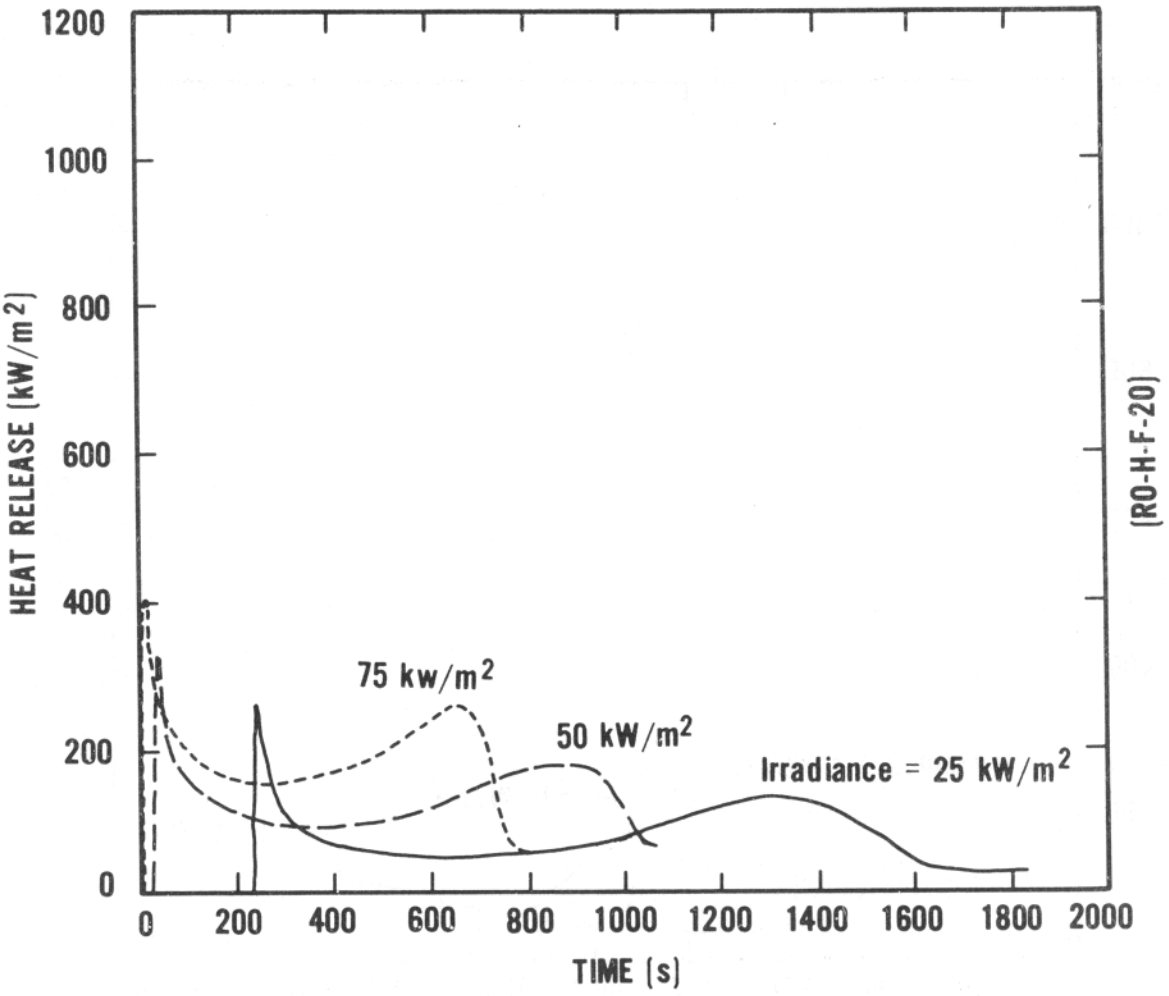

Figure 30. Red oak (horizontal rate of heat release at several irradiances

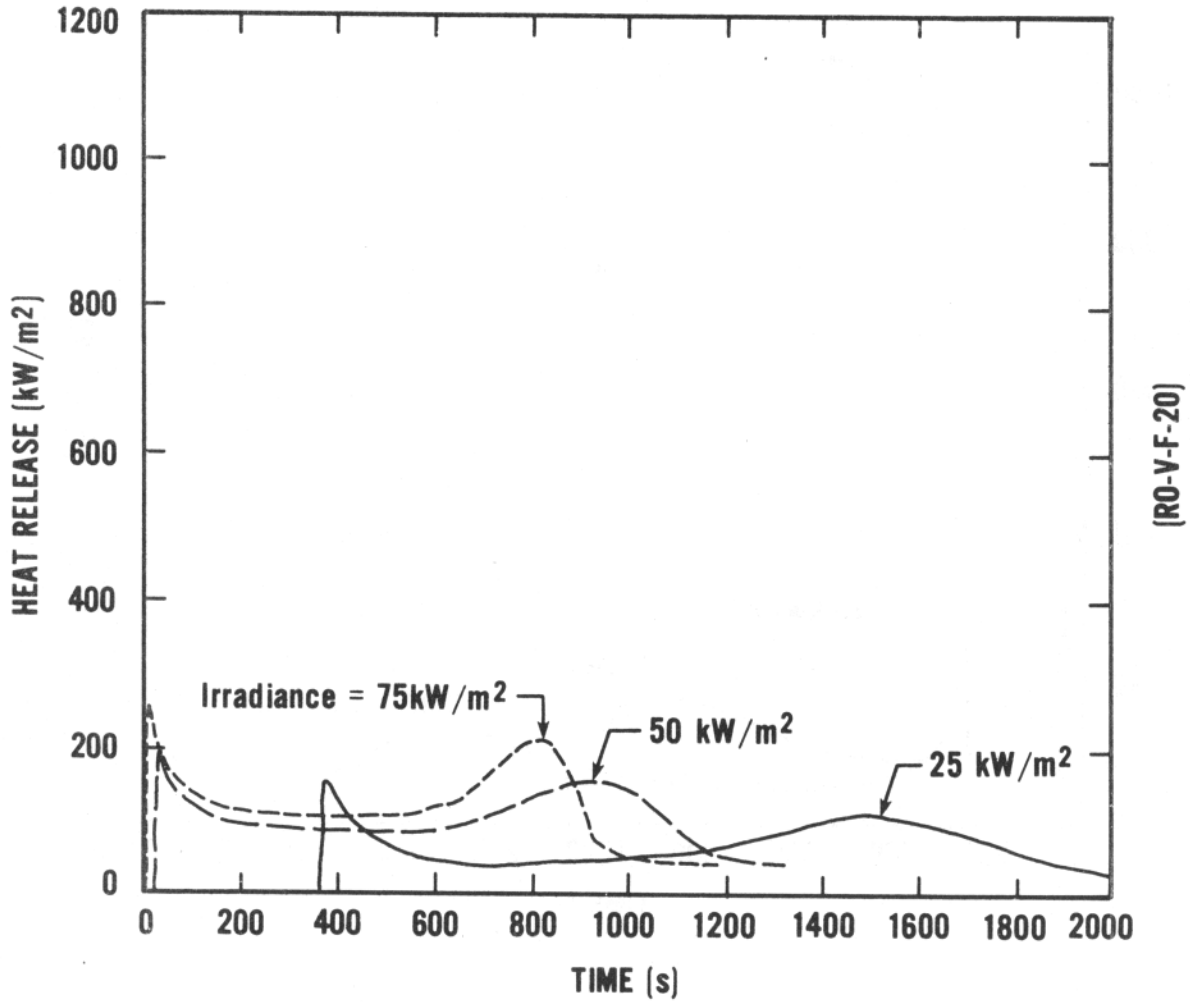

Figure 31. Red oak (vertical) rate of heat release at several irradiances

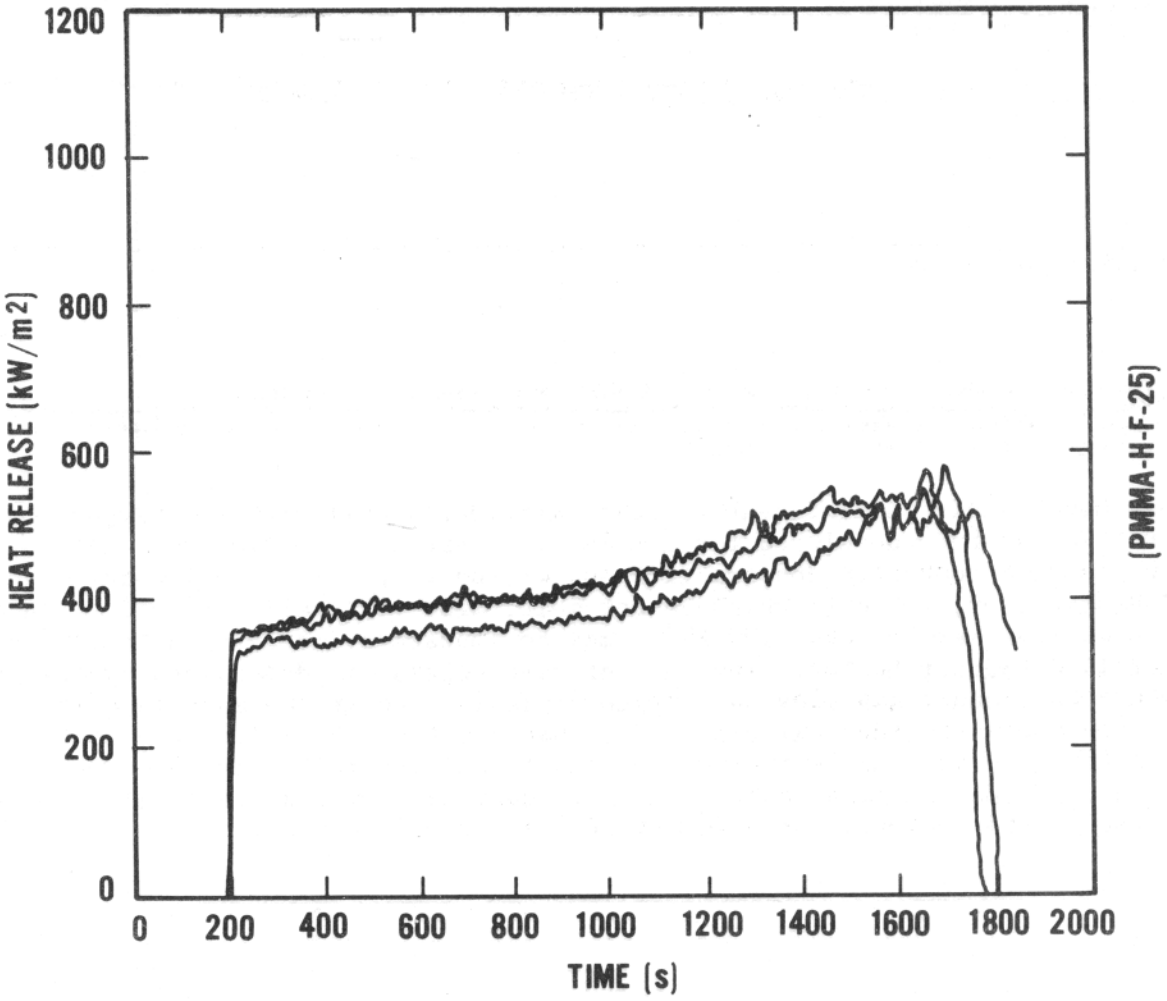

Figure 32. PMMA (horizontal) variations during three runs at 25 kW/m^2 irradiance

NBS-114A (REV. 2-80)

U.S. DEPT. OF COMM. BIBLIOGRAPHIC DATA SHEET (See instructions)	1. PUBLICATION OR REPORT NO. NBSIR 82-2611	2. Performing Organ. Report No.	3. Publication Date November 1982

4. TITLE AND SUBTITLE

Development of the Cone Calorimeter -- A Bench-Scale Heat Release Rate Apparatus Based on Oxygen Consumption

5. AUTHOR(S)

Vytenis Babrauskas

6. PERFORMING ORGANIZATION *(If joint or other than NBS, see instructions)*

NATIONAL BUREAU OF STANDARDS
DEPARTMENT OF COMMERCE
WASHINGTON, D.C. 20234

7. Contract/Grant No.

8. Type of Report & Period Covered

9. SPONSORING ORGANIZATION NAME AND COMPLETE ADDRESS *(Street, City, State, ZIP)*

10. SUPPLEMENTARY NOTES

☐ Document describes a computer program; SF-185, FIPS Software Summary, is attached.

11. ABSTRACT *(A 200-word or less factual summary of most significant information. If document includes a significant bibliography or literature survey, mention it here)*

A new bench-scale rate of heat release calorimeter utilizing the oxygen consumption principle has been developed for use in fire testing and research. Specimens may be of uniform or composite construction and may be tested in a horizontal, face-up orientation, or, for ones which do not melt, also vertically oriented. An external irradiance of zero to over 100 kW/m^2 may be imposed by means of a temperature-controlled radiant heater. The rate of heat release is determined by measuring combustion product gas glow and oxygen depletion, while the mass loss is simultaneously recorded directly. The instrument has been designed to be capable of higher accuracy than existing instruments and yet to be simple to operate and moderate in construction cost. The instrument is termed a "cone calorimeter" because of the geometric arrangement of the electric heater.

12. KEY WORDS *(Six to twelve entries; alphabetical order; capitalize only proper names; and separate key words by semicolons)*

calorimeters, combustion, fire tests, heat of combustion, heat release rate, ignition, oxygen consumption, plastics

13. AVAILABILITY

☒ Unlimited

☐ For Official Distribution. Do Not Release to NTIS

☐ Order From Superintendent of Documents, U.S. Government Printing Office, Washington, D.C. 20402.

☒ Order From National Technical Information Service (NTIS), Springfield, VA. 22161

14. NO. OF PRINTED PAGES 84

15. Price $10.50

USCOMM-DC 6043-P80